

# Aging of Fiber Reinforced Elastomeric Bridge Bearings

**Andrea Calabrese, PhD**

**Arman Barjani**

**Nghiem Tran**



# MINETA TRANSPORTATION INSTITUTE

Founded in 1991, the Mineta Transportation Institute (MTI), an organized research and training unit in partnership with the Lucas College and Graduate School of Business at San José State University (SJSU), increases mobility for all by improving the safety, efficiency, accessibility, and convenience of our nation's transportation system. Through research, education, workforce development, and technology transfer, we help create a connected world. MTI leads the four-university, MTI leads the four-university California State University Transportation Consortium funded by the State of California through Senate Bill 1.

MTI's transportation policy work is centered on three primary responsibilities:

## Research

MTI works to provide policy-oriented research for all levels of government and the private sector to foster the development of optimum surface transportation systems. Research areas include: bicycle and pedestrian issues; financing public and private sector transportation improvements; intermodal connectivity and integration; safety and security of transportation systems; sustainability of transportation systems; transportation / land use / environment; and transportation planning and policy development. Certified Research Associates conduct the research. Certification requires an advanced degree, generally a Ph.D., a record of academic publications, and professional references. Research projects culminate in a peer-reviewed publication, available on TransWeb, the MTI website (<http://transweb.sjsu.edu>).

## Education

The Institute supports education programs for students seeking a career in the development and operation of surface transportation systems. MTI, through San José State University, offers an AACSB-accredited Master of Science in Transportation Management and graduate certificates in Transportation Management, Transportation Security, and High-Speed Rail Management that serve to prepare the nation's transportation managers for the 21st century. With the

active assistance of the California Department of Transportation (Caltrans), MTI delivers its classes over a state-of-the-art videoconference network throughout the state of California and via webcasting beyond, allowing working transportation professionals to pursue an advanced degree regardless of their location. To meet the needs of employers seeking a diverse workforce, MTI's education program promotes enrollment to under-represented groups.

## Information and Technology Transfer

MTI utilizes a diverse array of dissemination methods and media to ensure research results reach those responsible for managing change. These methods include publication, seminars, workshops, websites, social media, webinars, and other technology transfer mechanisms. Additionally, MTI promotes the availability of completed research to professional organizations and journals and works to integrate the research findings into the graduate education program. MTI's extensive collection of transportation-related publications is integrated into San José State University's world-class Martin Luther King, Jr. Library.

---

## Disclaimer

The contents of this report reflect the views of the authors, who are responsible for the facts and accuracy of the information presented herein. This document is disseminated in the interest of information exchange. The report is funded, partially or entirely, by a grant from the State of California. This report does not necessarily reflect the official views or policies of the State of California or the Mineta Transportation Institute, who assume no liability for the contents or use thereof. This report does not constitute a standard specification, design standard, or regulation.

REPORT 19-05

# **AGING OF FIBER REINFORCED ELASTOMERIC BRIDGE BEARINGS**

Andrea Calabrese, PhD  
Arman Barjani  
Nghiem Tran

May 2019

A publication of

**Mineta Transportation Institute**

Created by Congress in 1991

College of Business  
San José State University  
San José, CA 95192-0219

# TECHNICAL REPORT DOCUMENTATION PAGE

<b>1. Report No.</b> 19-05	<b>2. Government Accession No.</b>	<b>3. Recipient's Catalog No.</b>	
<b>4. Title and Subtitle</b> Aging of Fiber Reinforced Elastomeric Bridge Bearings		<b>5. Report Date</b> May 2019	
		<b>6. Performing Organization Code</b>	
<b>7. Authors</b> Calabrese, Andrea <a href="https://orcid.org/0000-0001-7441-9275">https://orcid.org/0000-0001-7441-9275</a>		<b>8. Performing Organization Report</b> CA-MTI-1863	
<b>9. Performing Organization Name and Address</b> Mineta Transportation Institute College of Business San José State University San José, CA 95192-0219		<b>10. Work Unit No.</b>	
		<b>11. Contract or Grant No.</b> ZSB12017-SJAUX	
<b>12. Sponsoring Agency Name and Address</b> State of California SB1 2017/2018 Trustees of the California State University Sponsored Programs Administration 401 Golden Shore, 5th Floor Long Beach, CA 90802		<b>13. Type of Report and Period Covered</b> Final Report	
		<b>14. Sponsoring Agency Code</b>	
<b>15. Supplemental Notes</b>			
<b>16. Abstract</b> <p>Elastomeric bearings for thermal deformations and base isolation are used increasingly worldwide. Rubber-based devices have proven to be an effective passive protection system capable of reducing earthquake-induced forces in both the upper and the lower structures of bridges and buildings. Degradation of the bearings due to aging and environmental conditions may jeopardize their load carrying capacity, energy dissipation characteristics, and effectiveness when used as bearing pads or as base isolators. Among other environmental factors, degradation of rubber bearings is due to a variety of reasons, including, solar radiation, ozone, wind, salt water, and acid rain attacks, in addition to dynamic strain of long duration. To improve the reliability of laminated rubber bearings it is of paramount importance to understand the aging characteristics of these devices and their long-term performance both in compression and shear. While it is generally accepted that the degradation of polymers occurs as a nonuniform or heterogeneous process, detailed mechanical models including long-term degradation effects of rubber bearings used in bridges are not available. With this consideration in mind, the aim of this project is that of investigating the durability of Fiber Reinforced Bearings (FRBs) under long-term degradation, and that of assessing the modification of their axial and shear force-deformation response induced by aging effects. The study of the long-term performance of elastomeric bearings used in bridges will not only help addressing long-term road and bridge maintenance needs, but it also constitutes an invaluable contribution towards the understanding of the response of existing infrastructures under seismic loads.</p>			
<b>17. Key Words</b> Bridge bearings; structural engineering	<b>18. Distribution Statement</b> No restrictions. This document is available to the public through The National Technical Information Service, Springfield, VA 22161		
<b>19. Security Classif. (of this report)</b> Unclassified	<b>20. Security Classif. (of this page)</b> Unclassified	<b>21. No. of Pages</b> 60	<b>22. Price</b>

Copyright © 2019  
by **Mineta Transportation Institute**  
All rights reserved

Mineta Transportation Institute  
College of Business  
San José State University  
San José, CA 95192-0219

Tel: (408) 924-7560  
Fax: (408) 924-7565  
Email: [mineta-institute@sjsu.edu](mailto:mineta-institute@sjsu.edu)

[transweb.sjsu.edu](http://transweb.sjsu.edu)

## ACKNOWLEDGMENTS

Funding for this research was provided by the State of California SB1 2017/2018 through the Trustees of the California State University (Agreement # ZSB12017-SJAUX) and the California State University Transportation Consortium.

The authors thank MTI staff, including Executive Director Karen Philbrick, Ph.D.; Deputy Executive Director Hilary Nixon, Ph.D.; Research Support Assistant Joseph Mercado; Executive Administrative Assistant Jill Carter; and Editing Press for editorial services.

**Cover image:** Corey Coyle, [https://commons.wikimedia.org/wiki/File:US\\_Highway\\_61\\_State\\_Highway\\_35\\_Overpass\\_-\\_panoramio.jpg](https://commons.wikimedia.org/wiki/File:US_Highway_61_State_Highway_35_Overpass_-_panoramio.jpg).

---

## TABLE OF CONTENTS

<b>Executive Summary</b>	<b>1</b>
<b>I. Introduction</b>	<b>2</b>
<b>II. Methodology</b>	<b>5</b>
<b>III. Experimental Tests on Fiber Reinforced Laminated Rubber Pads</b>	<b>6</b>
Introduction	6
Test Specimens	6
Experimental Setup for Compression and Shear Tests	7
Compression Tests	9
Shear Tests	14
<b>IV. Effects of Rubber Bearings Aging on the Seismic Response of a     Typical Base Isolated Overpass Bridge in California</b>	<b>24</b>
Description of the Benchmark Structure and Finite Element Model	24
Modelling of Rubber Bearings for NRHAs Including Aging Effects	27
Ground Motion Selection	34
Definition of the Intensity Measures (IMs) to be Used for the Analysis of the Structural Response	38
Results	39
<b>V. Conclusions</b>	<b>47</b>
<b>Abbreviations and Acronyms</b>	<b>49</b>
<b>Endnotes</b>	<b>50</b>
<b>Bibliography</b>	<b>54</b>
<b>About the Authors</b>	<b>58</b>
<b>Peer Review</b>	<b>59</b>

---

## LIST OF FIGURES

1. Samples of Neoprene FRBs	7
2. Universal Testing Machine with Test Fixture for Shear Tests of Rubber Devices	8
3. FRBs Spaced Apart in Air Oven for Curing	9
4. Time History of the Vertical Load for Compression Tests	10
5. Time History of the Vertical Load for Compression Tests – Dynamic Cycles	10
6. Vertical Load - Displacement Response	11
7. Vertical Load – Displacement Response	11
8. Vertical Load – DisplacementResponse	12
9. Secant Stiffness vs. Aging Time for Different Levels of Axial Load	14
10. Time-History of the Imposed Lateral Displacement	15
11. Horizontal Force vs. Horizontal Displacement at 50% Shear Strain – Week 3	16
12. Horizontal Force vs. Horizontal Displacement at 50% Shear Strain – Week 4	16
13. Horizontal Force vs. Horizontal Displacement at 50% Shear Strain – Week 5	17
14. Horizontal Force vs. Horizontal Displacement at 75% Shear Strain – Week 3	17
15. Horizontal Force vs. Horizontal Displacement at 75% Shear Strain – Week 4	18
16. Horizontal Force vs. Horizontal Displacement at 75% Shear Strain – Week 5	18
17. Common Failure Mechanism of Aged FRBs At 75% Shear Strain	19
18. Effective Stiffness at 50% Shear Strain vs. Aging Time	20
19. Energy Dissipated per Cycle at 50% Shear Strain vs. Aging Time	21
20. Equivalent Viscous Damping at 50% Shear Strain vs. Aging Time	22
21. Percentage Variation of Shear Stiffness at 50% Shear Strain	23
22. Elevation of the Bridge	24
23. Cross Section of the Deck of the Bridge	24

---

24. Schematic Description of the Finite Element Model of the Bridge	25
25. 3D View of the SAP2000 Model of the Bridge	25
26. Extruded View of the SAP2000 Model of the Bridge	26
27. Bilinear Hysteretic Model and Parameters	27
28. Flowchart of the Iterative Procedure for the Determination of the Parameters of the Bilinear Model	28
29. Nonlinear Response of the New Elastomeric Devices Considered in this Study	29
30. Effects of the Modification Factors on the Nonlinear Repose of a Base Isolation Device	33
31. Nonlinear Response of Aged Elastomeric Devices Considered in this Study	33
32. Epicentral Distance vs. Magnitude of the Events Selected for this Study	38
33. Elements for which the EDPs have been Determined	39
34. Peak Horizontal Displacement of the Isolator vs. PGV	41
35. Peak Axial Load on the Bearing vs. PGV	41
36. Peak Vertical Acceleration of the Deck vs. PGV	42
37. Peak column Base Shear vs. PGV	42
38. Peak Top Column Rotation vs. PGV	43
39. Peak Column Ductility Demand vs. PGV	43
40. Peak Horizontal Displacement of the Isolator vs. PGA	44
41. Maximum Axial Load on the Bearing vs. PGA	44
42. Peak Vertical Acceleration of the Deck vs. PGA	45
43. Peak Column Base Shear vs. PGA	45
44. Peak Top Column Rotation vs. PGA	46
45. Peak Column Ductility Demand vs. PGA	46

---

## LIST OF TABLES

1. Characteristic of the MTS Series 370 Servohydraulic Load Frame	8
2. Vertical Test Results for an Axial Pressure of 3.00 MPa	13
3. Vertical Test Results for an Axial Pressure of 3.45 MPa	13
4. Vertical Test Results for an Axial Pressure of 3.90 MPa	13
5. Procedure for Displacement-Controlled Tests of FRBs	15
6. Shear Test Results at 50% Shear Strain	21
7. Parameters of the Bilinear Model for the as New and Aged Response	29
8. Maximum Values of Aging $\Lambda$ -Factors for Elastomeric Isolators <sup>44</sup>	32
9. Summary of the Events Selected for the Analyses	35

## EXECUTIVE SUMMARY

Elastomeric bearings for thermal deformations and base isolation are used increasingly worldwide. Rubber-based devices have proven to be an effective passive protection system capable of reducing earthquake-induced forces in both the upper and the lower structures of bridges and buildings. Degradation of the bearings due to aging and environmental conditions may jeopardize their load carrying capacity, energy dissipation characteristics, and effectiveness when used as bearing pads or as base isolators. Among other environmental factors, degradation of rubber bearings is due to a variety of reasons, including, solar radiation, ozone, wind, salt water, and acid rain attacks, in addition to dynamic strain of long duration. To improve the reliability of laminated rubber bearings it is of paramount importance to understand the aging characteristics of these devices and their long-term performance both in compression and shear. While it is generally accepted that the degradation of polymers occurs as a nonuniform or heterogeneous process, detailed mechanical models including long-term degradation effects of rubber bearings used in bridges are not available. With this consideration in mind, the aim of this project is that of investigating the durability of Fiber Reinforced Bearings (FRBs) under long-term degradation, and that of assessing the modification of their axial and shear force-deformation response induced by aging effects. The study of the long-term performance of elastomeric bearings used in bridges will not only help addressing long-term road and bridge maintenance needs, but it also constitutes an invaluable contribution towards the understanding of the response of existing infrastructures under seismic loads.

---

## I. INTRODUCTION

Over the last decades, researchers have focused their attention on the study of Laminated Rubber Bearings (LRBs) and their degradation when exposed to a large set of environmental conditions. Degradation of the bearings modifies the stiffness and the energy dissipation characteristics of devices over time. For this reason, a considerable effort has been dedicated to studying and characterizing the development of heterogeneities and degradation of rubber bearings that result from aging. In 1992, Nakauchi analyzed small samples of a 100-year-old elastomeric bearing from a viaduct located in Australia which revealed that the aging of the elastomeric bearings was limited to the outside surface of the pads.<sup>1</sup> In 1995, Wise et al. reported that heterogeneous diffusion-limited oxidation occurs in rubber devices.<sup>2</sup> Such changes should be expected for many polymeric materials under accelerated aging conditions, such as exposure to high temperatures. In 1996, Watanabe et al. studied the 38-year-old natural rubber bearings of the Pelham Bridge.<sup>3</sup> The authors confirmed that oxidation is confined to some extent from the surface of the bearing, and that the horizontal stiffness of old natural rubber devices increases roughly 10% with time. In 1998 Celina et al. confirmed the effects of heterogeneous oxidation in natural rubber bearings at various temperatures.<sup>4</sup> In 2006, Itoh et al. performed a series of exposure tests on various rubber materials, including natural rubber, to explore the degradation effects induced by different environmental factors.<sup>5</sup> The authors showed that thermal oxidation is the predominant degradation factor in elastomers. They demonstrated that the speed and the extent of aging differs from the inner part of a rubber pad compared to its surface. A similar result was found adopting accelerated thermal oxidation tests on rubber blocks.<sup>6</sup> Other researchers studied aging effects on twenty year old rubber bearings, underlying the high durability of well manufactured elastomeric devices.<sup>7</sup> From the findings of the different works cited above, it is evident that degradation of rubber bearings is mostly confined to the external surface of the device, and the extent of degradation depends on the material properties of the rubber and on the manufacturing quality of the device itself.<sup>8</sup> This research focused on assessing the degradation of conventional elastomeric devices, where steel plates are used as reinforcement layers and an external rubber cover is used to protect steel reinforcements from the environment.

None of the research works cited above has addressed the degradation of FRBs. These bearings have been adopted in bridge engineering as they present significant advantages over conventional LRBs:

- They are lighter than LRBs, as the steel reinforcements are substituted with light fiber layers with similar mechanical properties.
- Each device can be easily produced to the required size and shape by cutting a pad of larger dimensions.<sup>9</sup>
- When unbonded to the top and bottom surface, the bearings can deform freely under shear loads. Tensile stresses in the layers of the bearings significantly reduce due to a stable and unrestrained roll over deformation.

Given these advantages over conventional devices, the applicability of FRBs as base isolators for bridges and residential buildings has been discussed in numerous studies.<sup>10, 11, 12</sup> Kelly and Calabrese derived closed form solutions to describe the vertical stiffness and the stress distribution in FRBs with differing shapes.<sup>13</sup> The 'pressure solution' takes into account the compressibility of the elastomer and the stretching of the fiber reinforcements. Various studies have confirmed that results of this analytical model match with sufficient approximation the vertical stiffness obtained from experimental testing.<sup>14</sup> A good agreement between experimental and analytical results was found for an average vertical pressure of 4.0 MPa. This vertical pressure represents the lower bound of the applied mean pressure in many bridge design codes.<sup>15</sup> An experimental study by Calabrese et al. has demonstrated that FRBs can perform well under seismic events representative of moderate to high seismic regions in Italy.<sup>16</sup> A study by Al-Anany and Tait has further focused on assessing the potential of FRBs when used in bridges. The study describes results of axial and lateral tests intended to replicate the loading conditions expected to occur during the lifetime of a bridge. The response of FRBs when a static rotation is applied to the top surface of the bearing is discussed as well. The rotation is intended to replicate the static deformation applied to the bearings due to long term deflection of simple supported bridges. The authors have found that static rotations reduce the vertical stiffness of the bearings under low levels of axial loads. Under large axial loads, vertical stiffness is not modified by an imposed static rotation.<sup>17</sup> FRBs were found to provide a stable response under rotational cyclic tests. The bearings were able to accommodate rotations that could result at the bridge/deck interface due to long term deformations of the superstructure.

While these bearings proved to be effective when adopted in both bridges and residential buildings, limited information is available on the time-dependent degradation of the devices due to their aging. To the best of the authors' knowledge, the only study on degradation of FRBs was carried out by Russo et al. This study includes the description of results of experimental tests on three pairs of aged FRBs. The aging protocol involved the curing of the devices in an oven at 70 °C for 21 days.<sup>18</sup> The procedure followed the specifications of the Italian seismic code.<sup>19</sup> The authors found that, due to aging, the average horizontal stiffness of FRBs increases of 15%, while the degradation of the energy dissipation characteristics of the devices was found to be influenced by the type of reinforcement layers in use. For devices with bidirectional carbon reinforcement layers, the authors have determined a reduction of equivalent viscous damping induced by aging of 20%. This reduction was found to be equal to 0.6% for devices with quadridirectional carbon fibers. The result underlines how the degradation of FRBs can be influenced by the degradation of the fiber reinforcements, and that a reduction of the energy dissipation characteristics of the bearings can be induced by the aging of devices.

In LRBs, the hardening induced by aging causes an increase in both the post-elastic stiffness and the characteristic strength of the bearing.<sup>20</sup> This means that due to aging, both the effective stiffness and the effective damping ratio of LRBs increase. Buckle et al. has found the increase of stiffness and equivalent viscous damping to be in the range of 10–20% over a 30-year period for low-damping rubber elements with a shear modulus between 0.5 and 1.0 MPa.<sup>20</sup> The scope of this work is that of shedding some light on the aging of FRBs. With this aim in mind, a large set of FRBs have been tested both in compression and shear after heat induced aging. Results for these tests have been compared to those available

in literature for conventional elastomeric devices. A bilinear model of hysteresis has been adopted to describe the effects of aging on the hysteretic response of these bearings. This model is used to describe the changes in stiffness, strength, and energy dissipation characteristic of rubber bearings caused by ageing. Nonlinear Response History Analyses (NRHAs) have then been performed to assess the influence of elastomeric bearing aging in the seismic response of a typical concrete overpass in California.

## II. METHODOLOGY

The aims of this research project include examining (i) the study of the long-term performance of bridge rubber bearings through testing and (ii) shedding some lights on the effects elastomeric bearing aging on the seismic response of a typical concrete overpass. A full range of available research techniques are embraced in this work, including experimental tests, numerical modelling of the devices and response history analyses of a typical bridge structure with aging of the rubber bearings explicitly modelled. Elastomeric bearings have been tested under axial and shear loads to verify the influence of aging on their mechanical response. Accelerated aging tests have been performed to determine the effects of thermal oxidation on the response of the bearings. This mechanism was found to be the single most important factor governing the aging behavior of vulcanized rubber devices.<sup>6</sup> The experimentally determined properties of FRBs have been compared to available results for conventional steel reinforced devices. Hysteresis models representative of new and aged reinforced fiber reinforced and steel reinforced bearings have been included in a structural model representative of an ordinary concrete bridge. Results of response history analyses of the prototype structure under tridirectional seismic excitation, including new and the aged devices, have been studied to verify the influence of aged elastomeric bearings on the global response of the structure. Multidirectional NRHAs were necessary for a complete understanding of the behavior of the prototype bridge under earthquake loads.

---

### III. EXPERIMENTAL TESTS ON FIBER REINFORCED LAMINATED RUBBER PADS

#### INTRODUCTION

As demonstrated by Kelly, low-cost rubber bearings can be produced using natural rubber and fiber reinforcements.<sup>9</sup> Fiber layers seem to be an ideal reinforcement for rubber bearings: they offer excellent corrosion resistance, high stiffness to weight ratio, good fatigue properties, ease of transportation, and handling.<sup>21</sup> Oxidation of rubber has been determined to be the single most significant factor influencing the aging characteristics of LRBs. The degradation of mechanical properties associated with oxidation of elastomeric components have been verified in elements exposed to room temperature along with low levels of oxidation. The rate of degradation of LRBs is significantly influenced by aging conditions, heat and light exposure, temperature levels, pressure, and exposed surface area.<sup>22</sup> For elastomeric bearings, exposed areas are generally limited to the lateral surface of the device, which is often smaller than the area of the bearing protected from the elements. For the reasons discussed in the introduction, the degradation tests considered in this study only consisted of heat-accelerated aging. Results of these tests have been used to predict the evolution of the mechanical properties of the bearings at ambient temperatures. Many standardized procedures are available to determine acceptable aging levels in rubber elements. For instance, AASHTO M251-06 specifies the duration and temperature levels at which rubber samples need to be exposed before shear and tensile tests are performed.<sup>23</sup> The mechanical properties of aged samples are then compared to those that are not aged. For natural rubber elements, heat resistance requirements in AASHTO M251-06 for ASTM D 573-04 allow a maximum change in durometer hardness of +10% in the shore A scale, and a maximum reduction of tensile strength and ultimate elongation of -25% after an aging time of 7 days at 70°C.<sup>24</sup> For neoprene, the maximum allowed changes in material properties include a variation of +15% in durometer hardness in the shore A scale, a maximum reduction of tensile strength of -15%, and a variation of the ultimate elongation of -40% after an aging time of 70 hours at 100°C. Following the procedures described in these standards, tests are performed on small specimens where the oxidation effects are evident on the entire piece of elastomer. The tests aim to assess the variation of the mechanical properties of aged full-scale elastomeric bearings, rather than verifying the localized modifications of mechanical properties of the small rubber samples. With this aim in mind, following the procedures described in Report 449 of the National Cooperative Highway Research Program,<sup>25</sup> tests were performed on small-scale rubber bearings. Results of the tests on scaled samples have been used to extrapolate the variation of the mechanical properties of full-scale devices exposed to ambient temperatures, and to compare the response of fiber-reinforced devices against conventional steel reinforced ones.

#### TEST SPECIMENS

The bearings for this study were supplied by Cal Neva Supply Co, San Leandro, CA 94577, and manufactured by Kirkhill Manufacturing Company, Downey, CA 90241 following Caltrans specifications. As per specifications, laminated pads were made by bonding together elastomeric layers and fabric reinforcements. The layers of elastomer were made

using neoprene for at least 60 percent by volume of the total elastomeric compound. The elastomer had a shear modulus of  $0.76 \text{ MPa} \pm 0.07 \text{ MPa}$ . The bearings had a top and bottom uniform elastomeric cover of  $1/8$  inch. A fabric reinforcement layer was used every  $1/2$  an inch throughout the entire thickness of the device. The reinforcement was a single ply at the top and bottom surfaces of the pad and double ply within the pad. The fabric layers were woven from 100 percent glass fibers with an “E” type yarn, which contained continuous fibers. The minimum thread count in either direction was 25 threads per inch. The fabric had a breaking strength larger than  $140 \text{ kN/m}$ . Samples were cut to the required size by Cal Neva Supply Co. The cutting was performed by avoiding heating of the material and producing a smooth edge with no tears or visible signs of damage to the bearings. A total of 42 FRBs were manufactured and tested. The bearings had a height of  $51.5 \text{ mm}$  and base dimensions of  $51.5 \times 51.5 \text{ mm}$  (=base area of  $2652.25 \text{ mm}^2$ ). Figure 1 shows typical FRBs tested to determine the degradation of the devices.

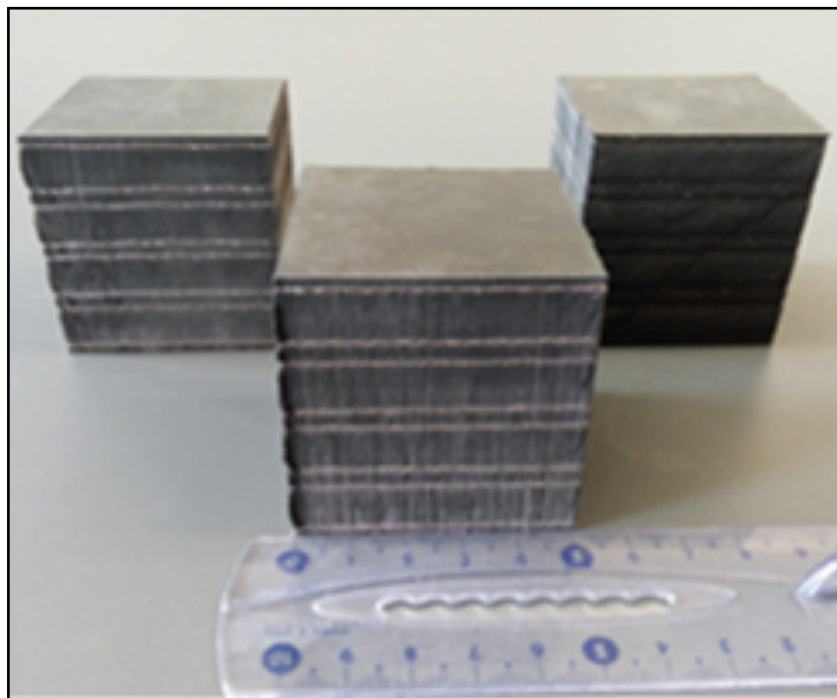


**Figure 1. Samples of Neoprene FRBs**

## **EXPERIMENTAL SETUP FOR COMPRESSION AND SHEAR TESTS**

An MTS Series 370 Servohydraulic Load Frame was used for the tests. The system provides versatility and high-performance solutions for accurate and repeatable static and dynamic material and component testing. The load frame is suitable to perform tests for compression and tension. It includes an axial hydraulic actuator with a maximum capacity of  $250 \text{ kN}$  ( $55 \text{ kip}$ ) and a stroke of  $150 \text{ mm}$  ( $6 \text{ in}$ ). Both displacement controlled, and force controlled procedures can be followed. In this configuration, the dynamic actuator is mounted on the upper crosshead, while a load cell is mounted below the lower hydraulic wedge. The data acquisition system along with the control of the hydraulic actuator are performed by a software running on a personal computer. The characteristics of the servohydraulic load frame are listed in Table 1.

**Table 1. Characteristic of the MTS Series 370 Servohydraulic Load Frame**

Axial Hydraulic Actuator Capacity	Stroke	Hydraulic Grip System	Data Acquisition
[kN]	[mm]	[MPa]	[-]
250 kN (55 kip)	150 mm (6 in)	70 (10000 psi)	16 bit at 5KHz max

Figure 2 shows the testing machine and the different components for shear testing. A classic double lap setup, shown in in Figure 2, was used for the tests. Samples were adhered to steel plates with an ethyl-based instant adhesive Loctite® 495 from Henkel after cleaning all the surfaces with a solvent produced by the same company. According to the Loctite® technical data sheet, the adhesive has a bonding time of 5 to 20 seconds when used to bond steel and neoprene. This is defined as the time required to develop a shear strength of 0.1 MPa. The full load carrying capacity of 1.0 MPa (measured as in ISO 4587) is developed after 24 hours at room temperature.<sup>26</sup> For pure compression tests, two 45 mm thick steel plates were fixed to the top and the bottom grips of the testing machine. The bearings were not bonded to the horizontal plates. The compression and shear tests were run at room temperature, while data was sampled at 250 Hz and filtered at 50 Hz.

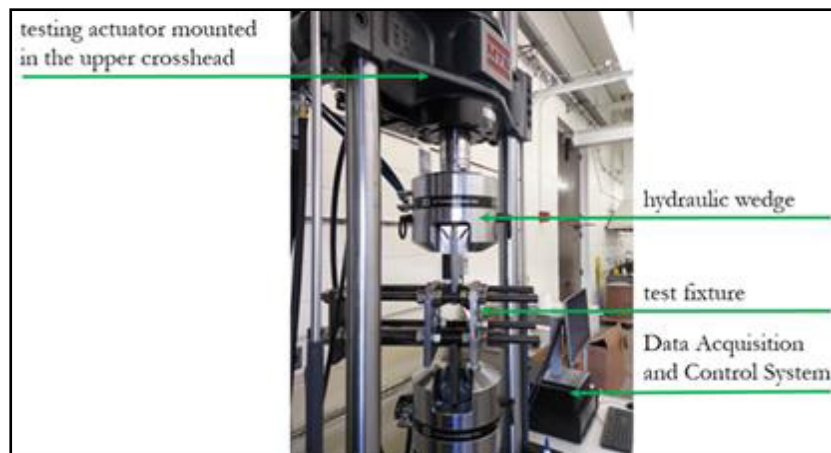


**Figure 2. Universal Testing Machine with Test Fixture for Shear Tests of Rubber Devices**

### Accelerated Aging

The majority of the accelerated aging tests described by international standards are performed on small samples where oxidation affects the performance of the whole specimen under tensile loads. With the aim of assessing the change in the overall stiffness and energy dissipation characteristic of a whole bearing, specimens of 51x51 mm were manufactured for compression and shear tests. The influence of specimen size on shear stiffness characteristics resulting from accelerated aging tests is discussed in full in Report 449 of the National Cooperative Highway Research Program.<sup>25</sup> For this work, all specimens were aged in an air oven wherein airflow and temperature were both controlled. The temperature of the oven was set at 100°C (212°F), and bearings were spaced apart and exposed on the entire surface for curing (see Figure 3). The bearings were tested after a curing time of 0, 1, 2, 3, 4, 5 and 6 weeks. Each device was removed from the oven one

day before testing, to allow for its cooling. All tests were performed at room temperature, ranging from 22°–24°C (71.6° to 75.2°F). With this combination of aging temperature and time, overheating or damage did not occur.



**Figure 3. FRBs Spaced Apart in Air Oven for Curing**

## **COMPRESSION TESTS**

The vertical stiffness of the bearings was obtained from compression tests carried out under load control. Loading histories for the vertical tests are presented in Figures 4 and 5. The bearings were initially loaded monotonically up to a design axial load of  $P = 8.9$  kN (this corresponds to a vertical pressure,  $\sigma_v$ , of 3.45 MPa). The vertical load was applied at a rate of 0.15 kN/s. After 60 seconds, three fully reversed sinusoidal cycles were imposed at 10 Hz. The amplitude of the sinusoidal cycles was set to  $\pm 3\%$  of  $P$  ( $=0.27$  kN). After the sinusoidal cycles, the bearings were monotonically unloaded. To assess the influence of the vertical load on the axial response of the bearings, the devices were tested at increasing values of vertical pre-loads, corresponding to a vertical pressure of 3.00, 3.45 and 3.90 MPa.

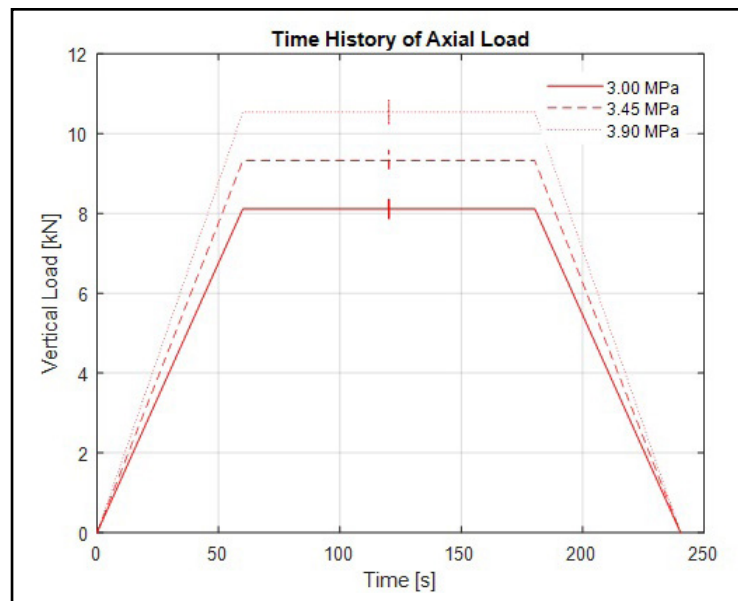


**Figure 4. Time History of the Vertical Load for Compression Tests**

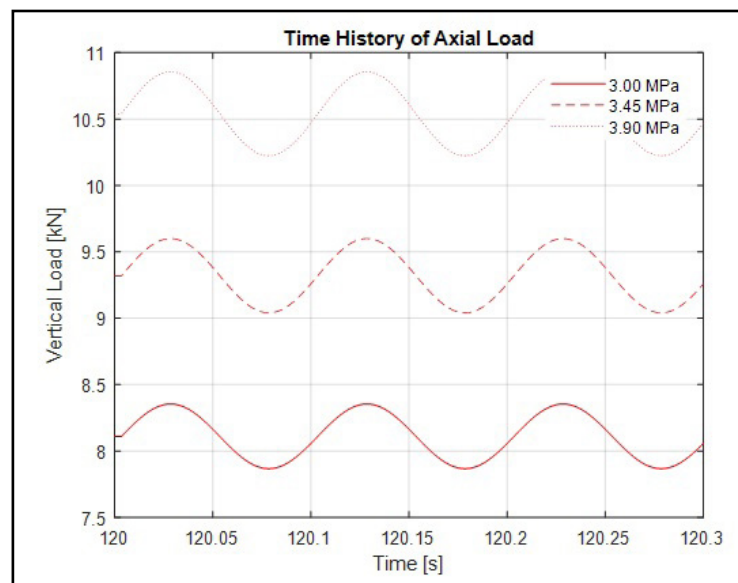


**Figure 5. Time History of the Vertical Load for Compression Tests – Dynamic Cycles**

### Summary of Results - Compression Tests

The static compression force–displacement curves for all the bearings for different levels of vertical preload and aging are shown in Figures 6–8. A visual inspection confirmed no signs of damage to the bearings after testing.

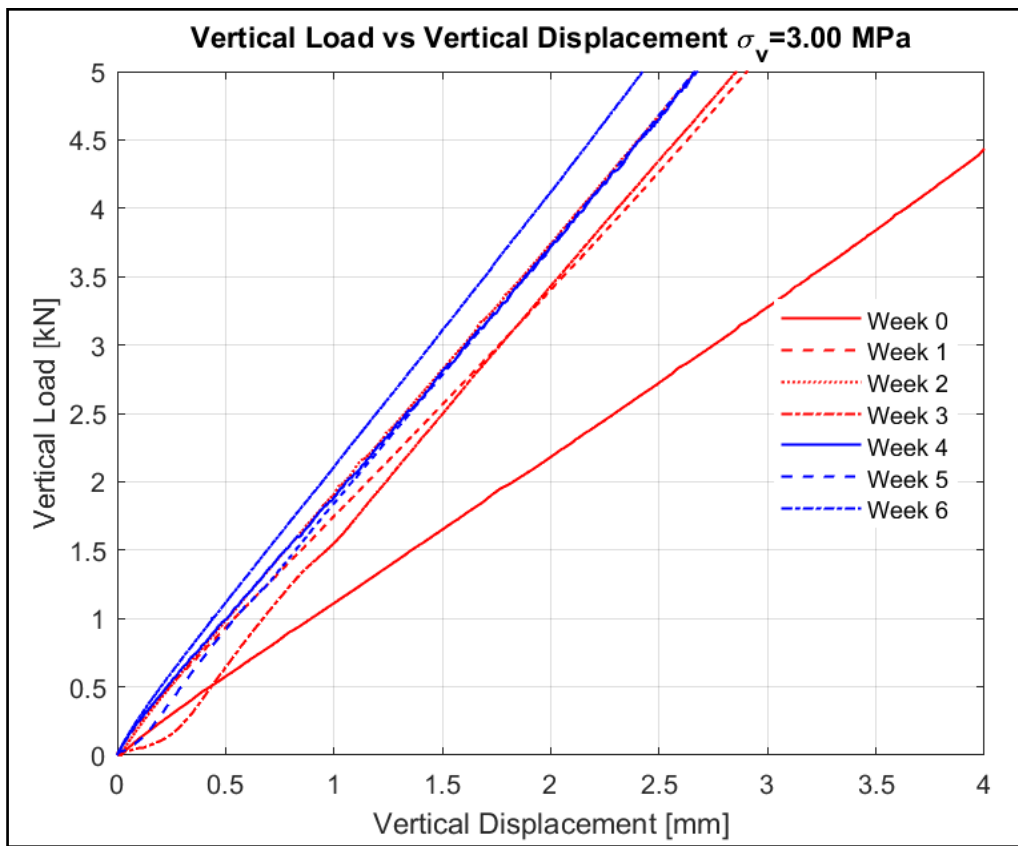


Figure 6. Vertical Load - Displacement Response (maximum pressure = 3.00 MPa)

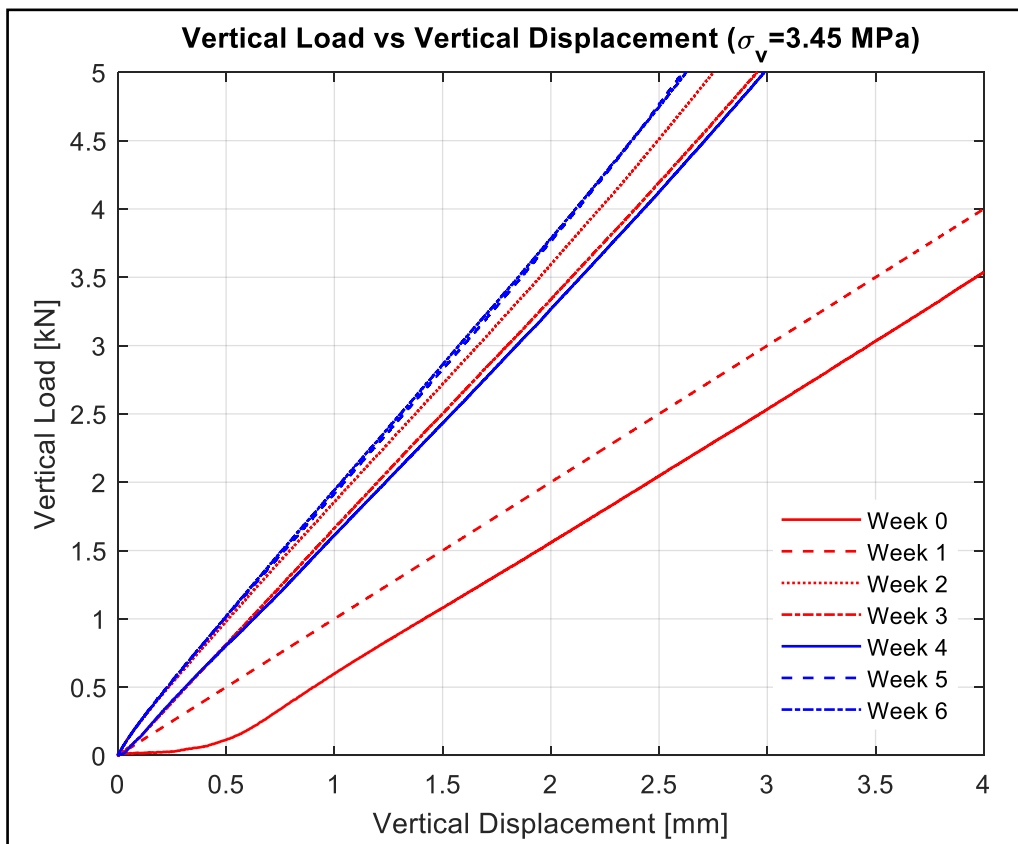
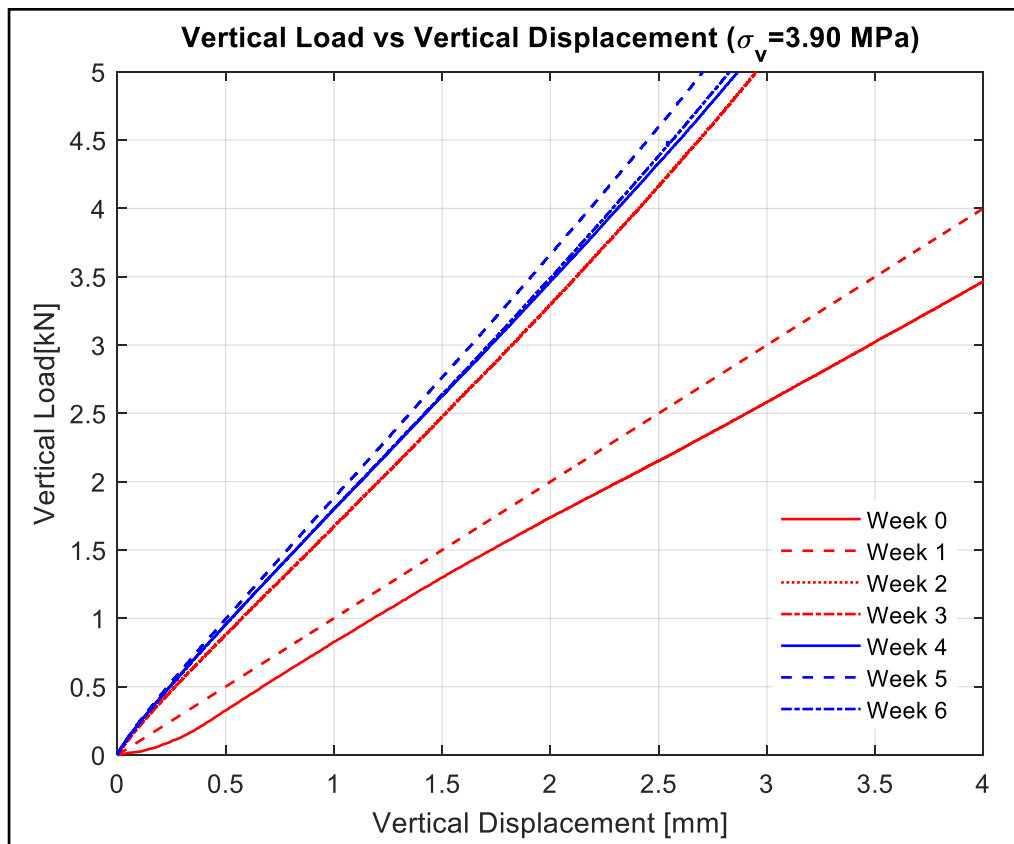


Figure 7. Vertical Load – Displacement Response (maximum pressure = 3.45 MPa)



**Figure 8. Vertical Load – Displacement Response (maximum pressure = 3.90 MPa)**

From previous experimental tests on FRBs it was found that compressive stress-strain curves for these bearings are highly nonlinear with significant run-ins before full vertical stiffness was developed. This nonlinear response is due to the nonlinearity of the elastomer in compression,<sup>27</sup> and to a peculiar behavior of FRBs underlined by Kelly: when FRBs are loaded in compression, the load is distributed to the horizontal reinforcements, the lack of straightness in the fiber layers is responsible of an initial low stiffness of the bearings under axial loads.<sup>10</sup> To reduce the run-in effect, an orthogonal in plane tension could be applied to the bi-directional reinforcements before bonding these fibers to the elastomeric layers. In other words, prestressing of the fiber layers could be used to eliminate the run-in effect.<sup>28</sup> Compared to what was found in previous research work, the devices tested for this study showed a linear behavior with limited run-in effects under gravity loads. Results of vertical tests are given in Table 2 to Table 4. The tables provide the average and the standard deviation of the secant stiffness of the bearings at peak pressure  $K_{p0}$ , the vertical frequency  $f_v$ , and the effective compression modulus,  $E_c$ , defined as

$$E_c = \frac{P}{Ae_c}$$

Given the vertical stiffness  $K_p$ , of the bearing under the vertical pressure  $p$ , the vertical frequency  $f_v$ , can be calculated as

$$f_v = \frac{1}{2p} \sqrt{\frac{K_p g}{pA}}$$

where  $A$  is the plan area of the specimen and  $g$  is the acceleration of gravity.

According to results, outlined in Tables 2–4, the bearings have vertical frequencies of approximately 5 Hz at week 0. After six weeks of aging, the vertical frequency of the devices increased to 7 Hz.

**Table 2. Vertical Test Results for an Axial Pressure of 3.00 MPa**

Specimen	Secant Stiffness [kN/mm]		Compression Modulus, $E_c$ [MPa]	Vertical Frequency [Hz]
	AM	$\sigma$		
Week 0	0.92	0.006	17.90	5.37
Week 1	1.00	0.006	19.42	5.59
Week 2	1.77	0.007	34.28	7.42
Week 3	1.77	0.006	34.30	7.43
Week 4	1.75	0.008	34.01	7.40
Week 5	1.86	0.007	36.17	7.63
Week 6	1.80	0.008	34.90	7.49

**Table 3. Vertical Test Results for an Axial Pressure of 3.45 MPa**

Specimen	Secant Stiffness [kN/mm]		Compression Modulus, $E_c$ [MPa]	Vertical Frequency [Hz]
	AM	$\sigma$		
Week 0	1.03	0.006	20.05	5.29
Week 1	1.00	0.006	19.42	5.21
Week 2	1.79	0.007	34.76	6.97
Week 3	1.70	0.006	33.03	6.80
Week 4	1.71	0.008	33.22	6.82
Week 5	1.90	0.007	36.97	7.19
Week 6	1.88	0.008	36.41	7.14

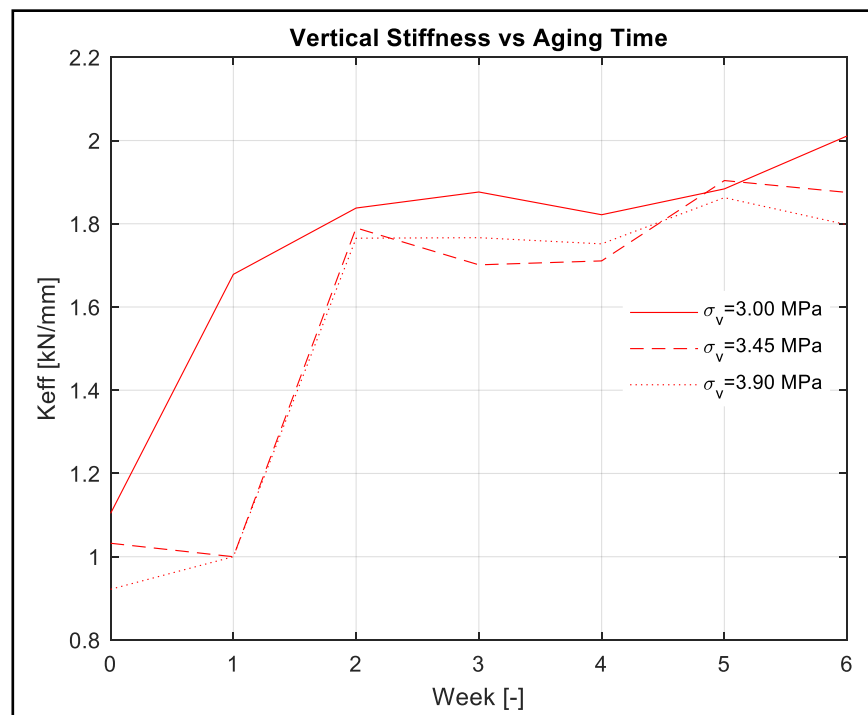
**Table 4. Vertical Test Results for an Axial Pressure of 3.90 MPa**

Specimen	Secant Stiffness [kN/mm]		Compression Modulus, $E_c$ [MPa]	Vertical Frequency [Hz]
	AM	$\sigma$		
Week 0	1.10	0.006	21.44	5.15
Week 1	1.68	0.006	32.59	6.35
Week 2	1.84	0.007	35.68	6.64

**Table 4, continued**

Specimen	Secant Stiffness [kN/mm]		Compression Modulus, $E_c$ [MPa]	Vertical Frequency [Hz]
	AM	$\sigma$	AM	AM
Week 3	1.88	0.006	36.43	6.71
Week 4	1.82	0.008	35.37	6.62
Week 5	1.88	0.007	36.58	6.73
Week 6	2.01	0.008	39.05	6.95

The results listed in Tables 2 to 4 confirm an increase in stiffness and  $E_c$  with increasing pressure and curing time. The behavior is nonlinear with the pressure; as the compression increases, the fiber sheets tend to straighten out the fiber strands, thus increasing the effective fiber stiffness. Figure 9 is a plot of the secant vertical stiffness of the bearings versus aging time at different levels of axial load.

**Figure 9. Secant Stiffness vs. Aging Time for Different Levels of Axial Load**

## SHEAR TESTS

The test setup for displacement controlled shear tests is shown in Figure 2. The time-history of the imposed lateral displacements is shown in Figure 10. During shear tests, FRBs were tested to 4 levels of increasing deformation amplitudes, corresponding to a 50%, 75%, 100%, and 150% shear strain. Three cycles of lateral displacement were imposed to the bearings for each level of lateral deformation. This procedure was defined to test the response of the bearings under displacement amplitudes resulting from earthquake shakings. Table 5 describes the test protocols used.

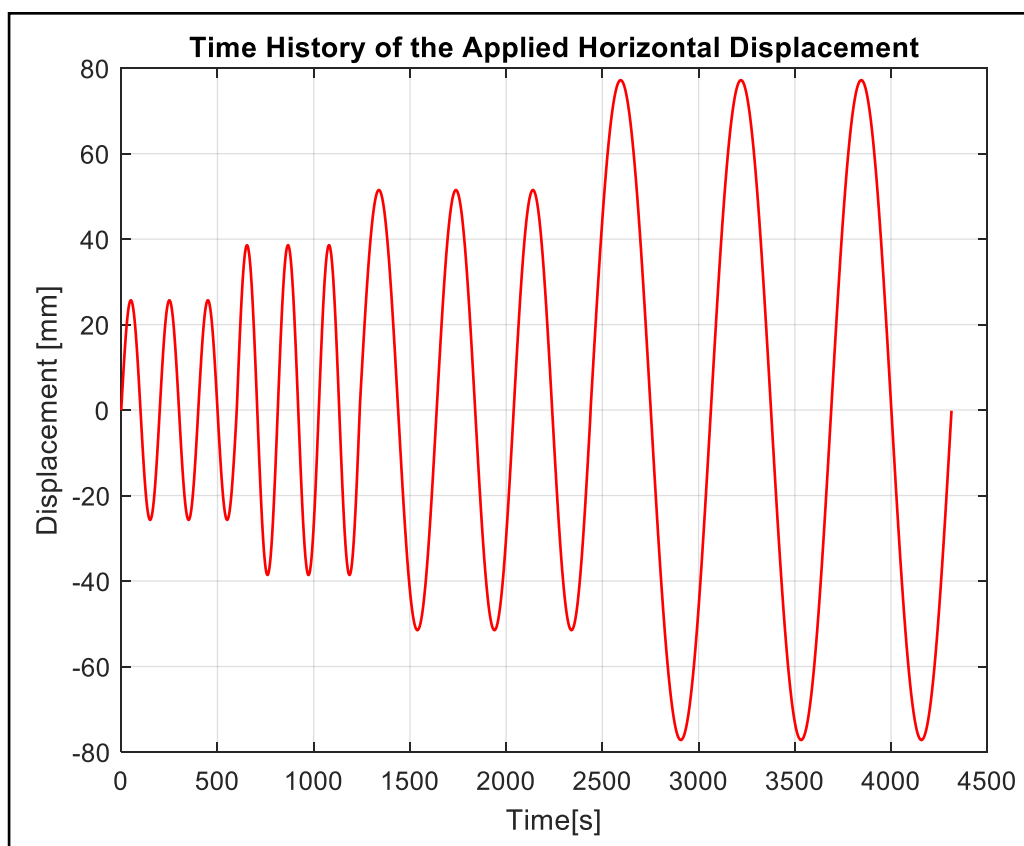


**Figure 10. Time-History of the Imposed Lateral Displacement**

During the tests, the bearings were deformed at a rate of 1% strain/second, and the force–displacement loops were recorded. From these tests, the effective horizontal stiffness, effective shear modulus, and viscous damping of the device were determined.

**Table 5. Procedure for Displacement-Controlled Tests of FRBs**

	Shear Displacement [mm]	Shear Deformation [%]	Frequency [Hz]	Maximum Estimated Horizontal Load [kN]
Test 1	25.7	50	0.0050	1.32
Test 2	38.6	75	0.0047	1.99
Test 3	51.5	100	0.0025	2.65
Test 4	77.2	150	0.0016	3.97

### Summary of Results – Shear Tests

After each week, six samples of FRBs were removed from the oven and tested. The force–displacement cycles measured at 50% shear strain after 3, 4, and 5 weeks of aging—as shown in Figures 11–13.

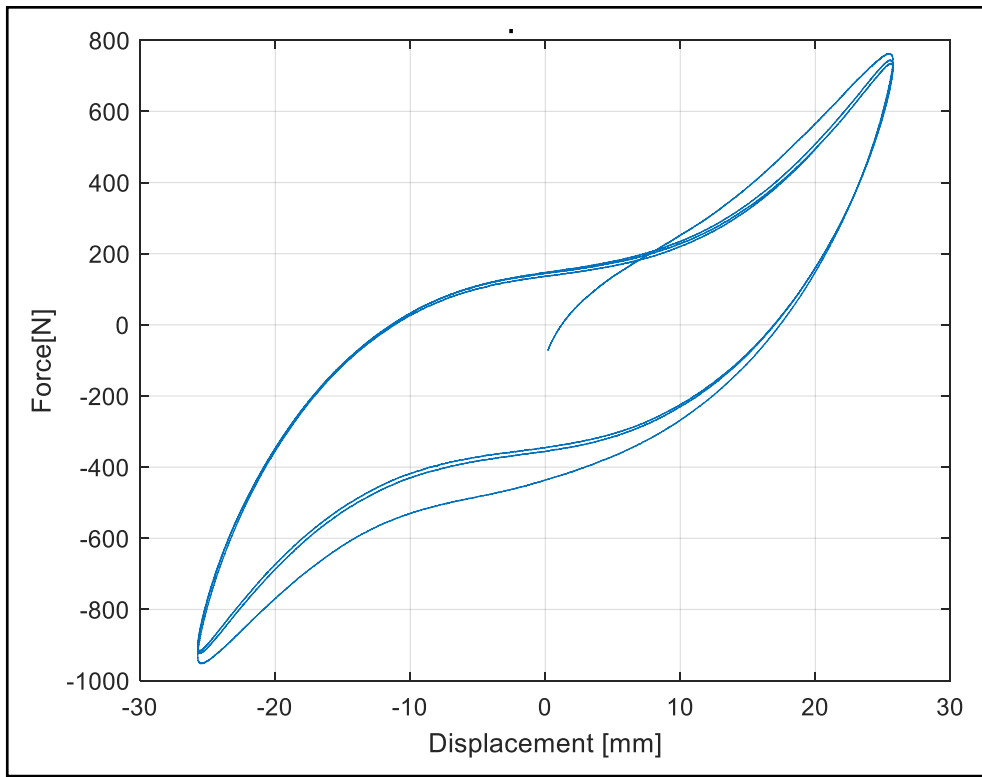


**Figure 11. Horizontal Force vs. Horizontal Displacement at 50% Shear Strain – Week 3**

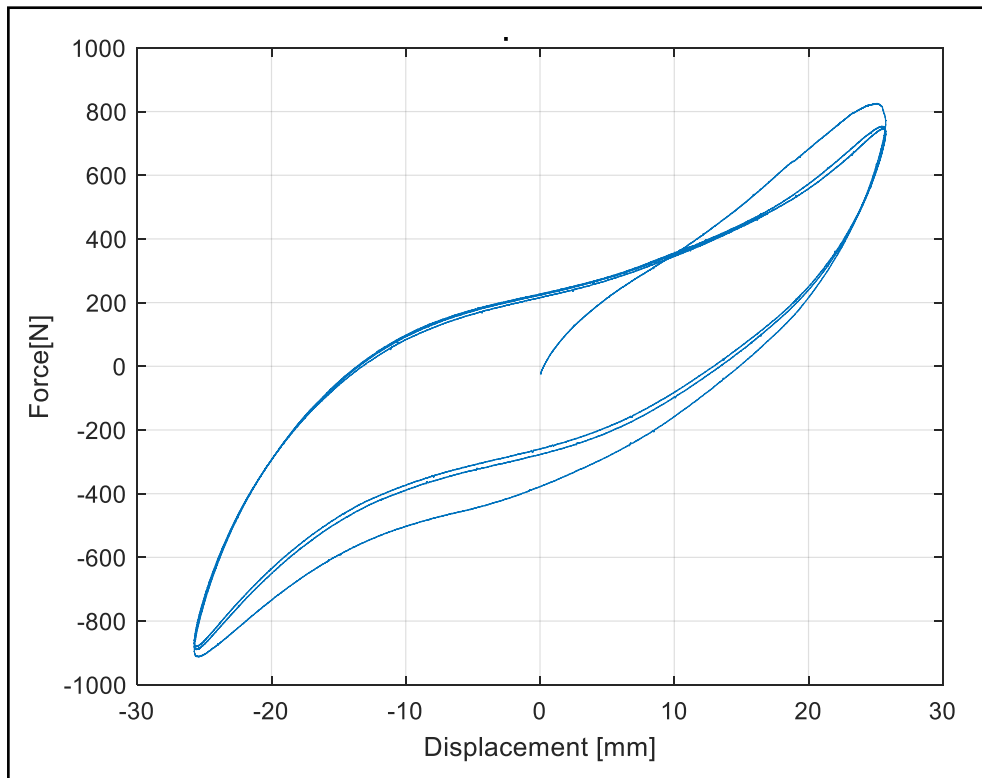


**Figure 12. Horizontal Force vs. Horizontal Displacement at 50% Shear Strain – Week 4**

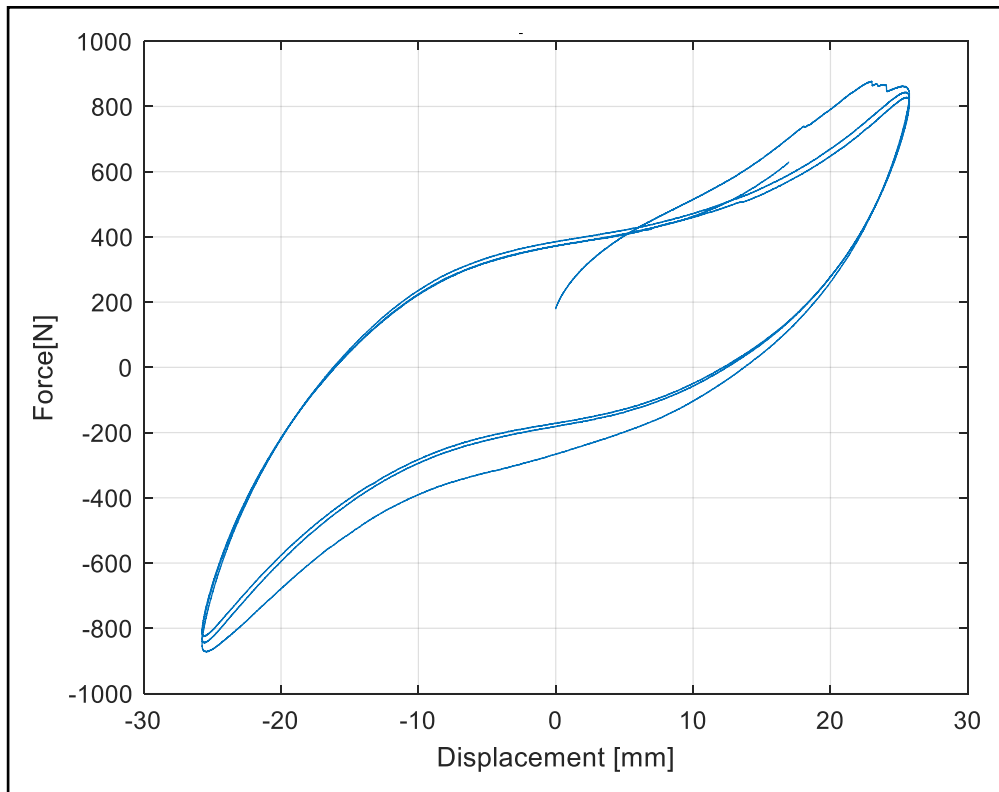


**Figure 13. Horizontal Force vs. Horizontal Displacement at 50% Shear Strain – Week 5**

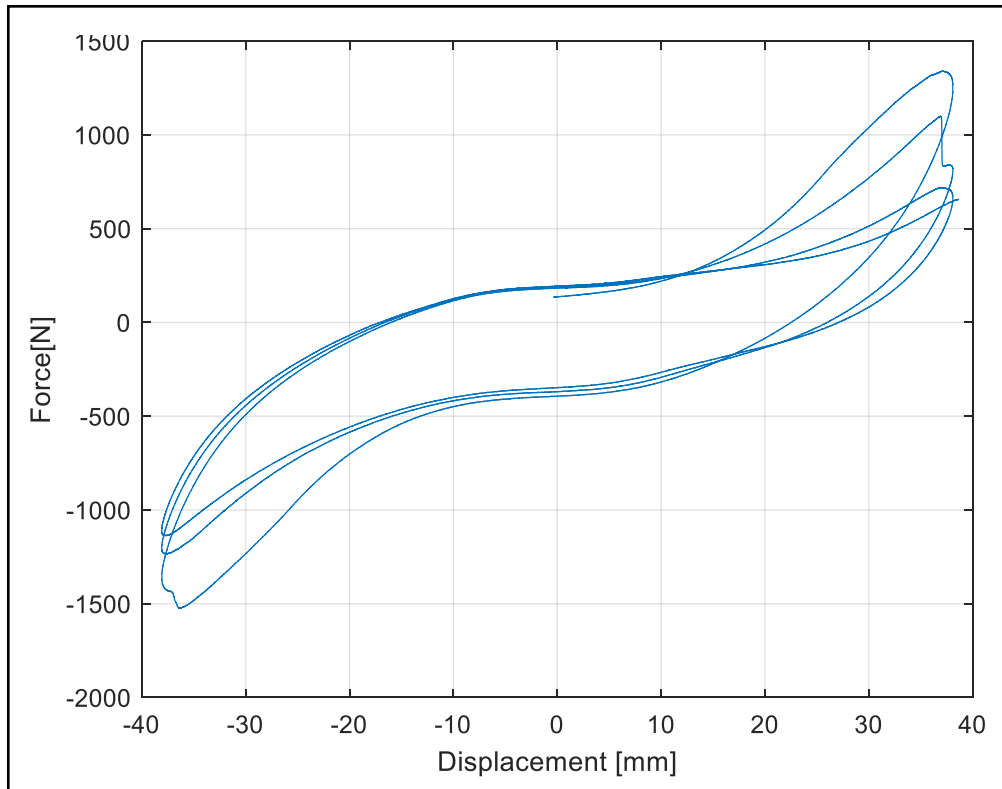


**Figure 14. Horizontal Force vs. Horizontal Displacement at 75% Shear Strain – Week 3**

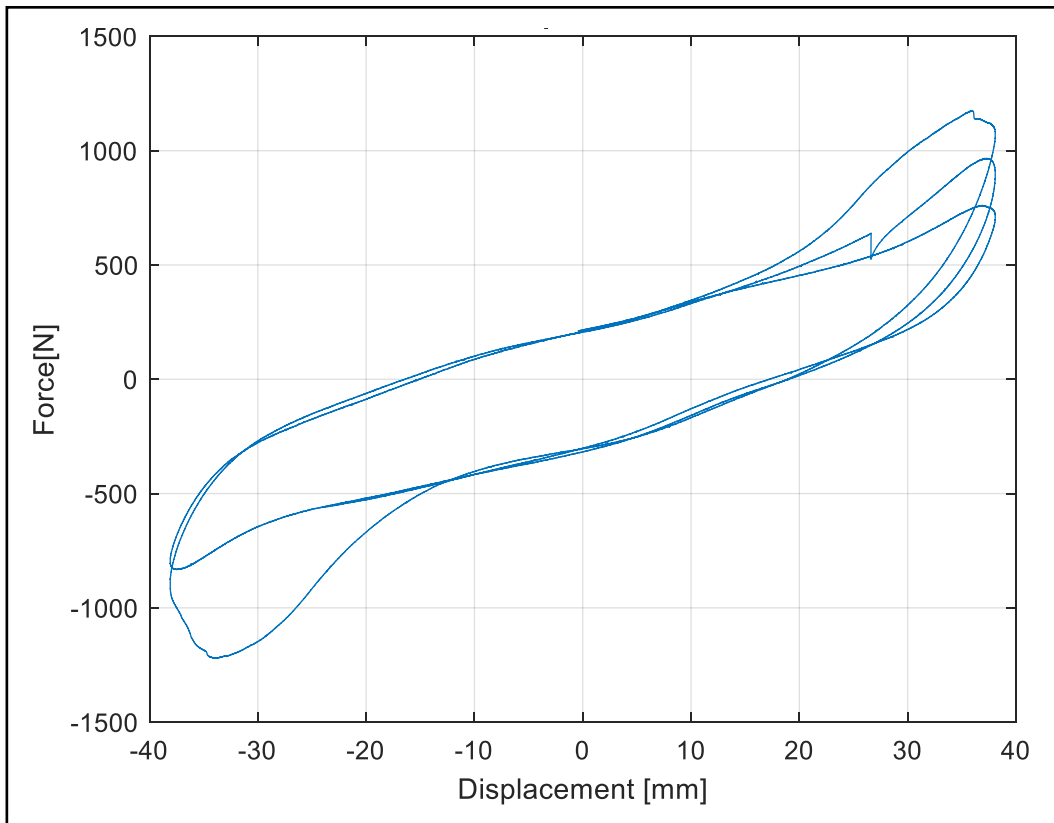


**Figure 15. Horizontal Force vs. Horizontal Displacement at 75% Shear Strain – Week 4**

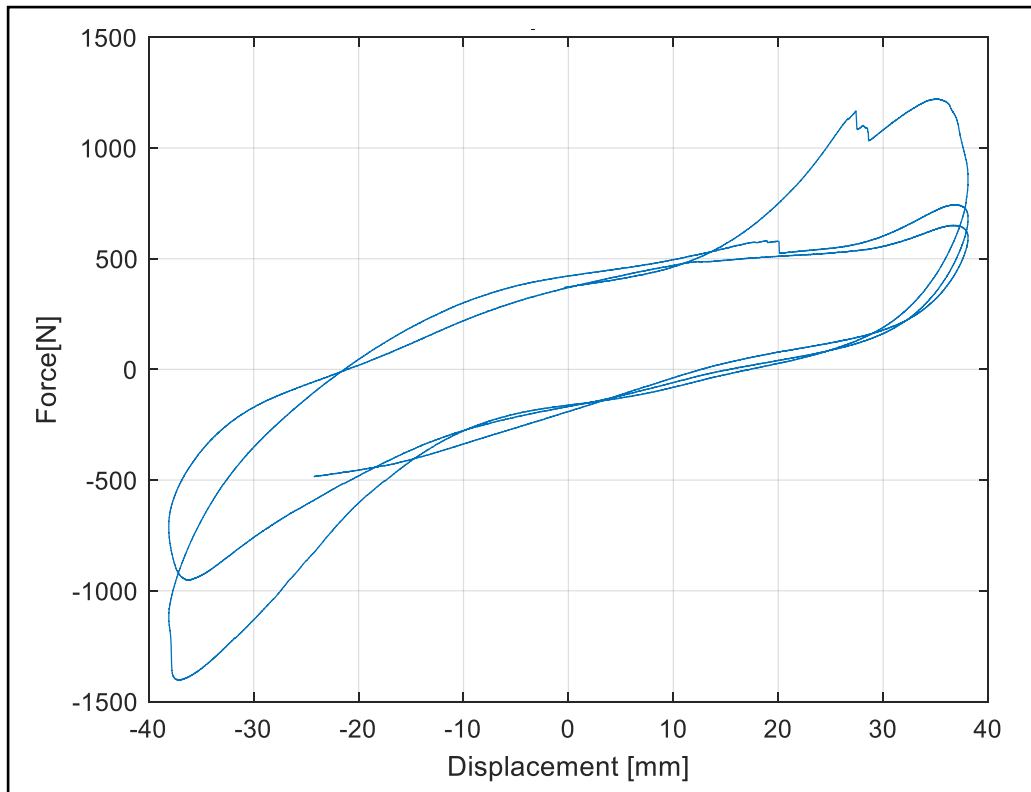


**Figure 16. Horizontal Force vs. Horizontal Displacement at 75% Shear Strain – Week 5**

Figures 14 to 16 show the force-displacement cycles measured at 75% shear strain after three, four, and five weeks of aging. As evidenced by the hysteresis loops, the stiffness of the bearings during the first cycle of deformation are larger than that exhibited during the following cycles of loading. A similar response is common in high damping elastomeric bearings where the initial stiffness is a measure of the response of the unscragged state of the elastomer (*i.e.*, a measure of the response of the ‘virgin’ material). After the first cycle of deformation, the bearing reaches the scragged state, a stable response that is manifested after the initial fracture of the molecules of elastomer.<sup>29</sup> When the bearings were tested to low levels of lateral deformation (*i.e.*, 50% shear strain), they showed a negligible degradation of the force displacement response. Contrarily, however, when these devices were tested to larger levels of lateral deformation (*i.e.*, shear strains larger than 75%), the measured hysteresis response showed degradation and softening of the devices after a few cycles of imposed displacements. Degradation of the response at 75% shear strain is shown in Figure 16 and demonstrates where the softening response was recorded. This softening response is not associated with the Mullins effect, which is the breakdown of weak bonds between rubber molecules and filler particles,<sup>30</sup> but is due to damage of the tested samples at the interfaces between the layers of elastomer and layers of fiber. The failure mechanism is shown in Figure 17.

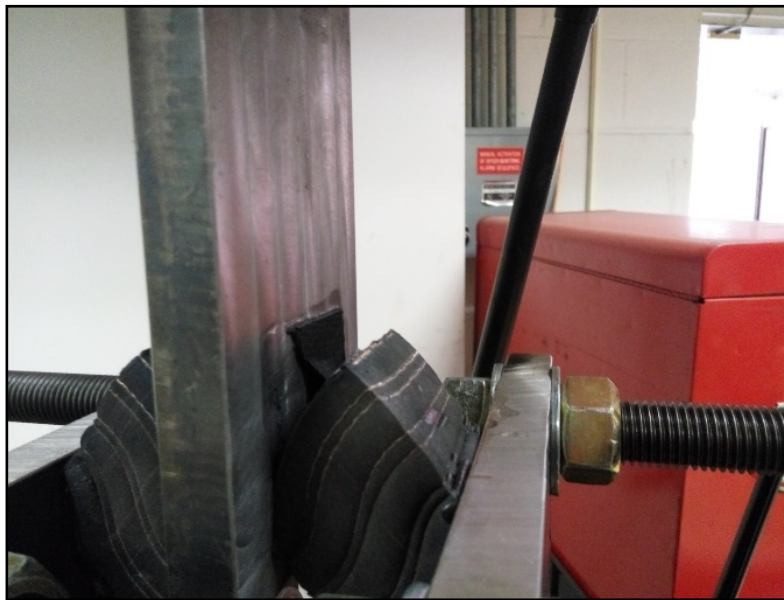


**Figure 17. Common Failure Mechanism of Aged FRBs At 75% Shear Strain**

The ethyl-based adhesive used to bond the bearings to the testing rig failed under shear deformations larger than 75%—though it should be noted that this only occurred in a few instances. This result confirmed the advantages of adopting fiber reinforced devices in unbonded configurations. When the bearings are unbonded, they are free to roll-off from the support. This reduces the tensile stresses at the edge of the bearings, which prevents the debonding of the different layers and damage of the devices under large lateral deformations. Results of shear tests on aged samples are given in this section for a shear strain of 50% only. This is because under large levels of lateral deformations, 35% of the tested bearings failed due to debonding of the composite device. The results shown in this section include the effective horizontal stiffness of the bearings  $k_{ij}$ , the shear

modulus of the elastomer  $G$ , the Energy Dissipated for each Cycle (EDC) of deformation and the equivalent viscous damping at various amplitudes of imposed displacements. From the tests, the effective lateral stiffness of the devices was calculated based on the peak-to-peak lateral response for each cycle of deformation as:

$$k_b = \frac{F_{\max} - F_{\min}}{\Delta_{\max} - \Delta_{\min}}$$

Results of the tests on FRBs are collected in Table 6 for a deformation amplitude of 26 mm, corresponding to a 50% shear strain, and different aging time. Figure 18 is a plot of the effective horizontal stiffness at 50% shear strain against aging time.

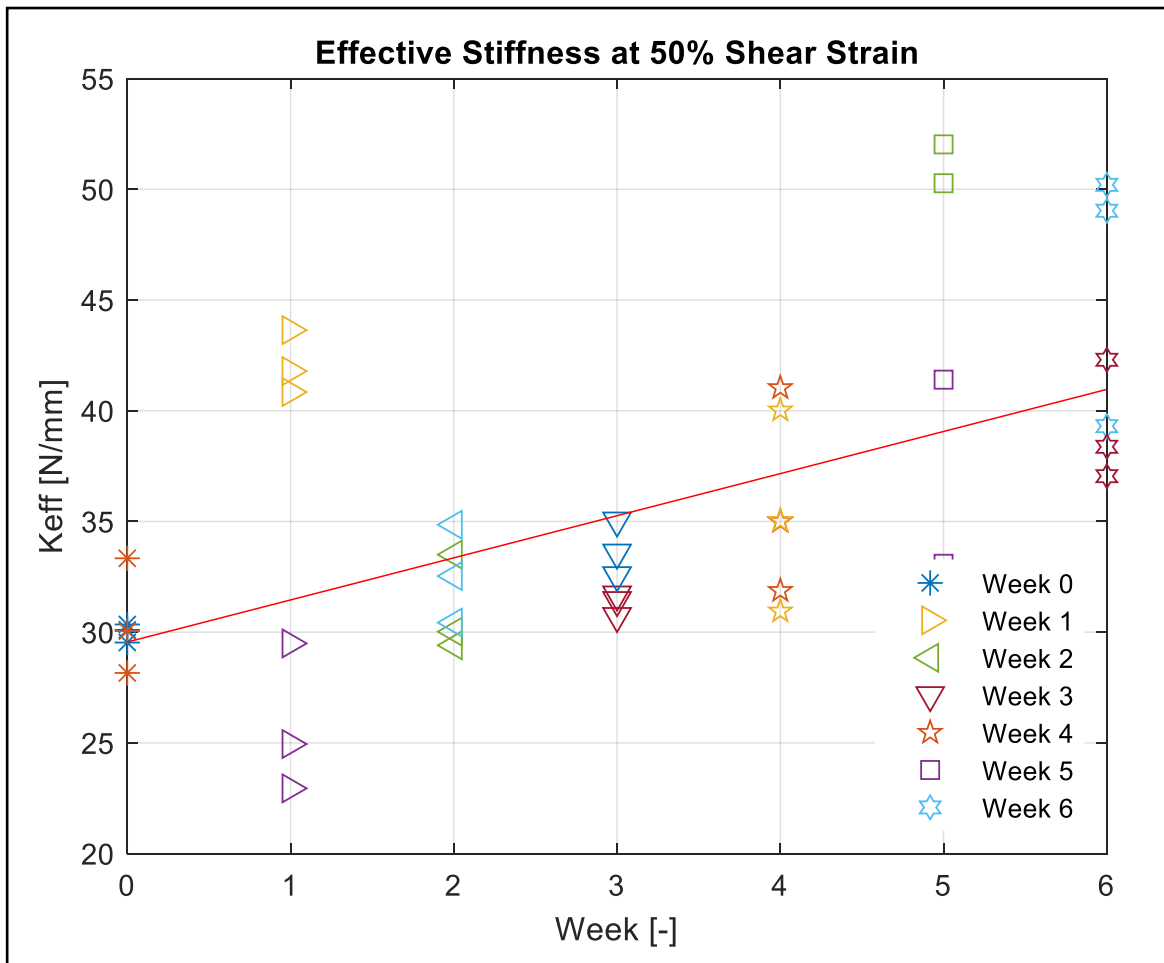


**Figure 18. Effective Stiffness at 50% Shear Strain vs. Aging Time**

In Figure 19 the EDC versus aging time is plotted for all the tested bearings. According to Figure 18, an increase in EDC was measured with aging time for a shear strain of 50%.

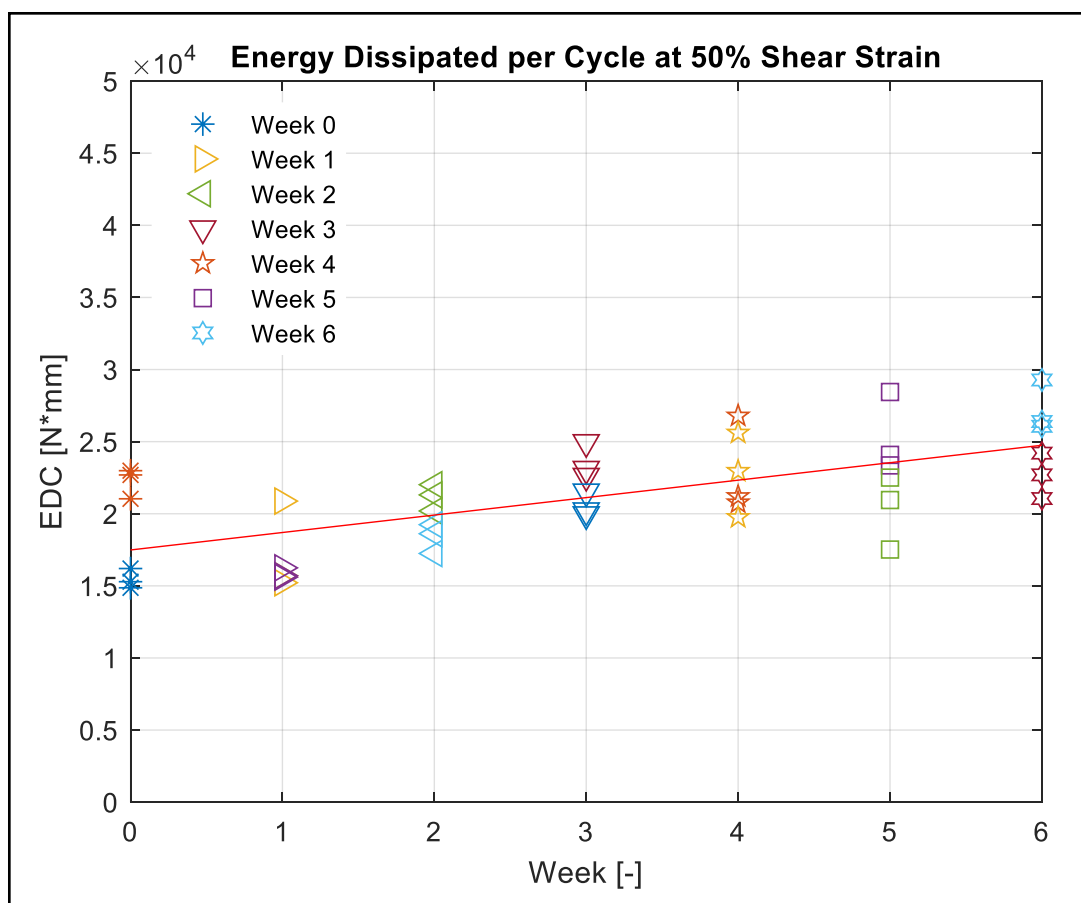


**Figure 19. Energy Dissipated per Cycle at 50% Shear Strain vs. Aging Time**

For elastomeric bearings, the shape of the hysteresis loops changes with repeated cycling. The response becomes stable after three cycles of imposed displacements.<sup>31</sup> For this reason, the property listed in Table 6 was obtained from the stable third cycle of hysteresis. The stabilized material properties obtained from the third cycle of hysteresis are often used by elastomeric bearing manufacturers to calculate material-property values.

**Table 6. Shear Test Results at 50% Shear Strain**

Week No.	EDC [N-mm]		$K_{b,Fmax}$ [N/mm]		$G$ [MPa]		$\chi$ [%]	
	AM	$\sigma$	AM	$\sigma$	AM	$\sigma$	AM	$\sigma$
0	18845	3800	30.26	1.70	0.58	0.03	0.16	0.04
1	16557	2142	33.94	9.22	0.65	0.18	0.12	0.04
2	19770	1765	31.79	2.17	0.61	0.04	0.15	0.02
3	22066	1890	32.51	1.58	0.63	0.03	0.16	0.02
4	22843	2820	35.65	4.13	0.69	0.08	0.15	0.03
5	22809	3611	39.96	9.45	0.77	0.18	0.15	0.05
6	24948	2927	42.71	5.64	0.82	0.11	0.14	0.02

For the tested bearings, an equivalent viscous damping between 12% to 16% of critical was measured at 50% shear strain. This result is in line with the findings of Kelly.<sup>11</sup> For full scale FRBs, the author found the equivalent viscous damping to be 15% of critical at 100% shear strain. Kelly found that when an unbonded FRB is deformed in shear, the bending of the fiber reinforcements causes planar cross sections not to remain planar. This deformation produces an interfacial slip of the fibers against each other in the threads, which generates a significant amount of frictional damping in the devices. For bonded FRBs, the deformation of the reinforcements due to bending is very limited, while the energy dissipation of the fiber layers due to frictional damping is negligible. The tests conducted for this study have found that a variation of aging time in the range of 0–6 weeks cause a variation of horizontal stiffness (*i.e.*, effective shear modulus) of around 41%, at a 50% shear strain. Under each level of imposed lateral deformations, the larger load-resisting capacity and damping were observed during the first cycles of deformation. For the following cycles at a 50% shear strain, the bearings exhibited a stable hysteresis loop. The equivalent viscous damping determined from testing is plotted in Figure 20 for various aging times.

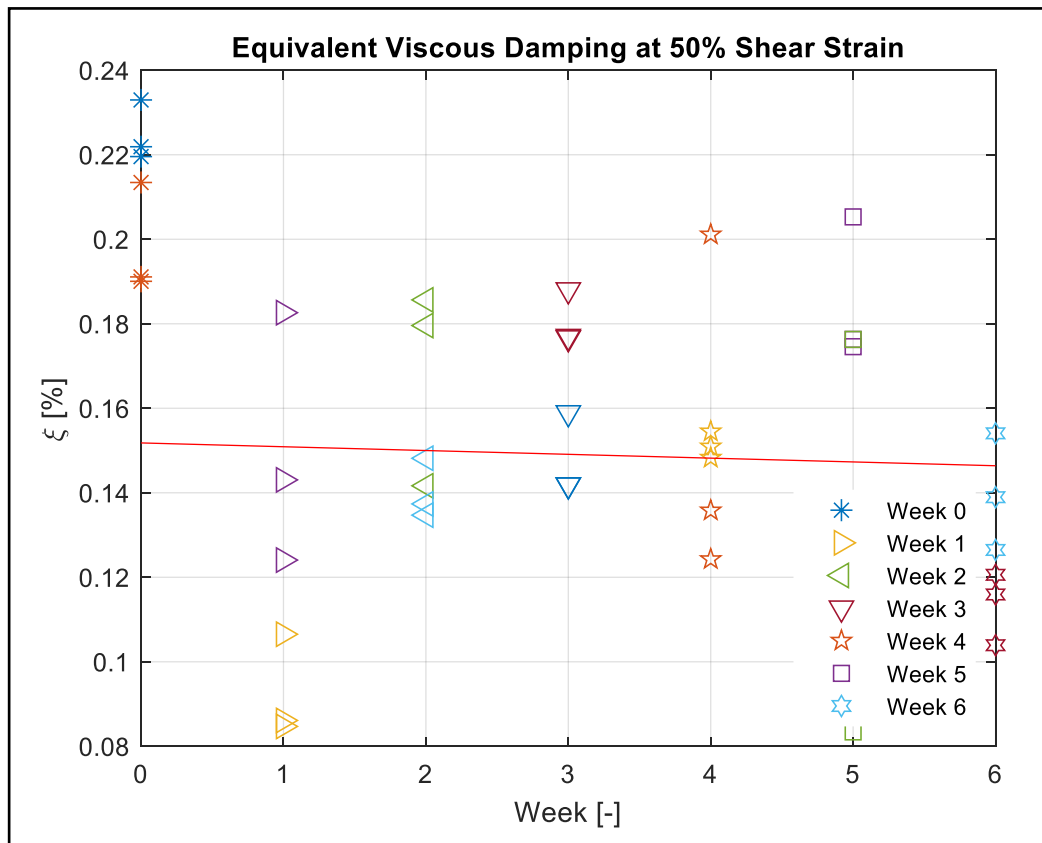


**Figure 20. Equivalent Viscous Damping at 50% Shear Strain vs. Aging Time**

Results of the tests performed on FRBs were compared to those obtained for steel reinforced elastomeric devices described in Report 449. The report collects the results of tests on conventional rubber bearings made from different types of Natural Rubber (NR100 and NR200) and neoprene rubber (NEO100 and NEO200). The samples of the 100 series had a shore A durometer of 50, the ones of the 200 series were made of 70 durometer

elastomers. The tests described in Report 449 follow the same protocol described in this report, for samples of the same dimensions.<sup>25</sup> Figure 21 is the plot of the percentage change in shear stiffness at 50% shear strain vs. aging time in days for the fiber reinforced and the steel reinforced bearings of Report 449. The change in percentage in stiffness (*i.e.*, secant shear modulus) is relative to the stiffness of the new device. The tests show that after six weeks of curing, the variation of lateral stiffness of FRBs due to aging is larger than that of steel reinforced devices. This result could be due to the degradation of fiber layers and the different manufacturing quality of tested bearings.

It is clear that the tests reported in this study are not sufficient for a full comparison of the response of FRBs against conventional elastomeric bearings. The high degradation of FRBs measured from the tests could be attributed to a different manufacturing quality of the samples or to the type of elastomer or fibers used. For a full understanding of any significant differences between the aging of conventional devices and fiber reinforced ones, it is necessary to test bearings produced by the same manufacturer, using the same elastomers and the same production procedures. The influence of different types of reinforcements on the aging response of FRBs should be assessed as well.

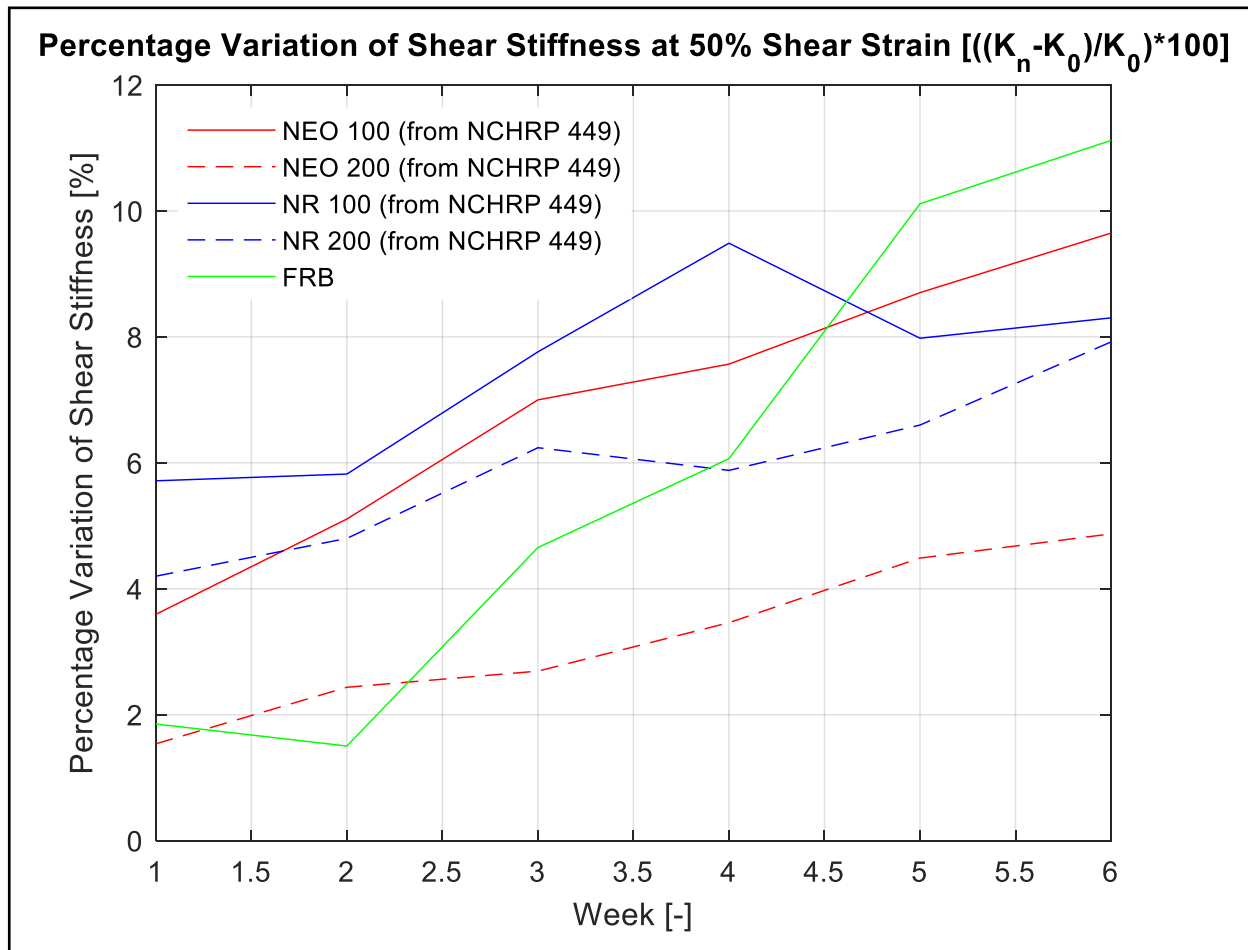


**Figure 21. Percentage Variation of Shear Stiffness at 50% Shear Strain**



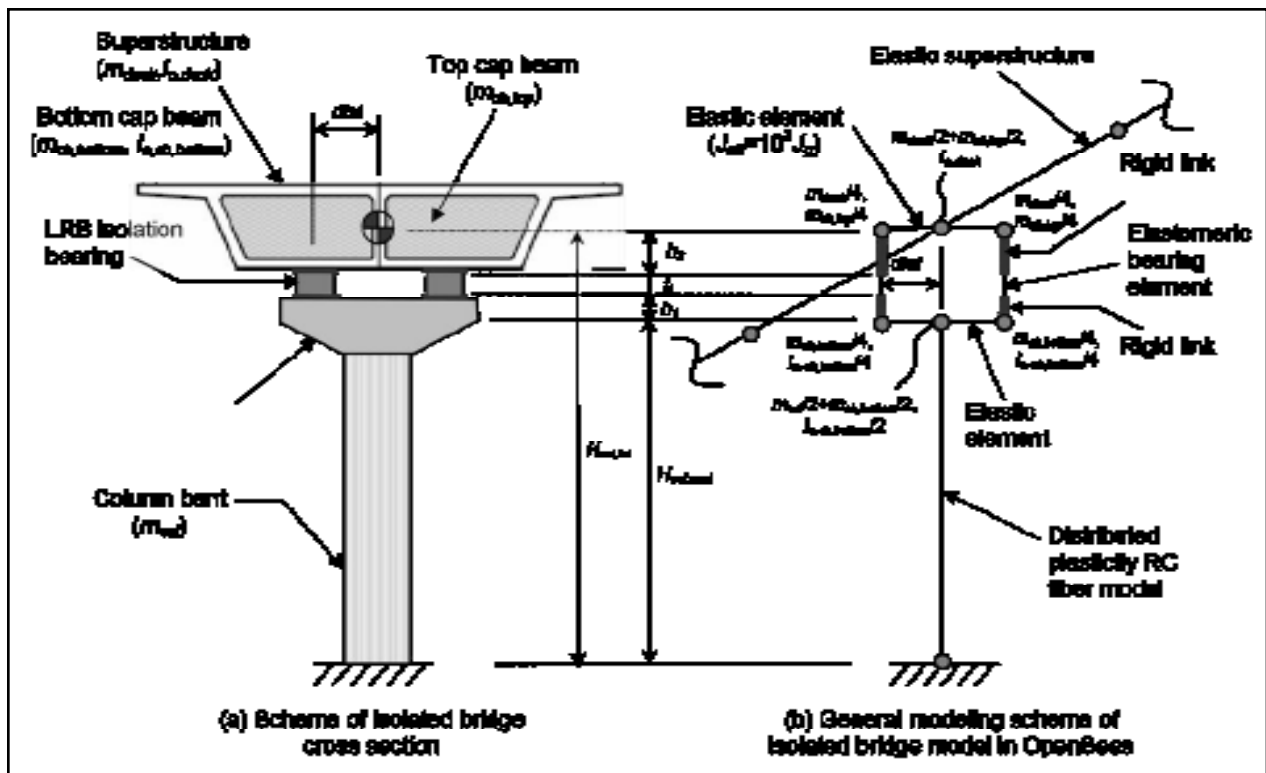


Figure 24. Schematic Description of the Finite Element Model of the Bridge<sup>34</sup>

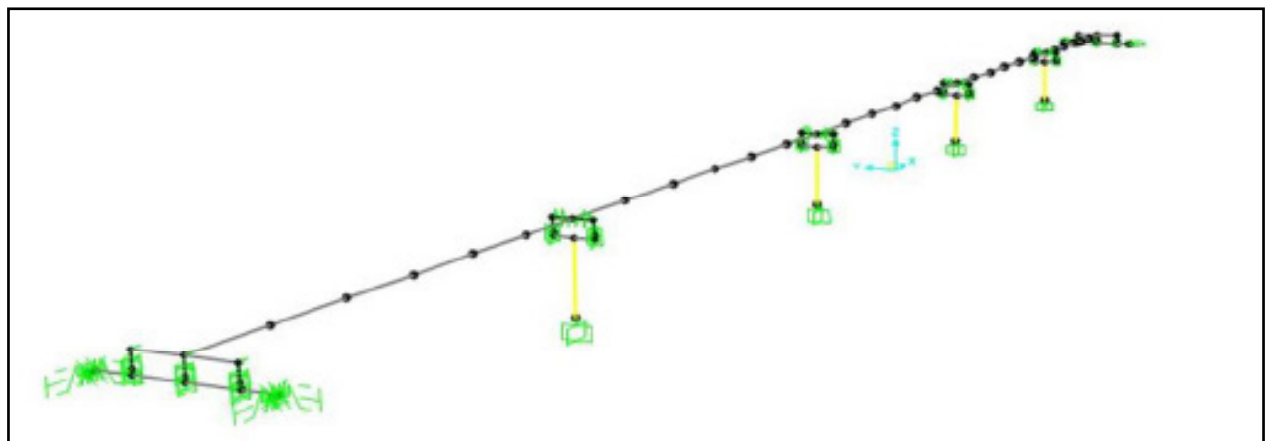
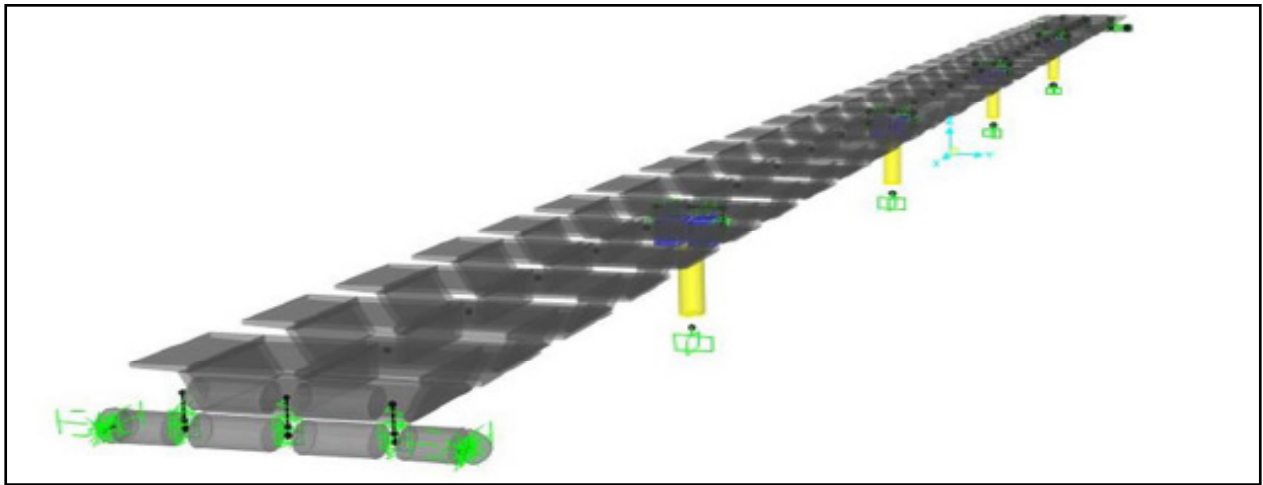


Figure 25. 3D View of the SAP2000 Model of the Bridge



**Figure 26. Extruded View of the SAP2000 Model of the Bridge**

The bridge was designed to AASHTO Standard Specifications for Highway Bridges and Caltrans Seismic Design Provisions.<sup>35,36</sup> The overpass has five spans and is fixed at the base. The columns of the bridge are modelled using a distributed plasticity element in SAP2000 and five integration points. Material models for concrete and steel were defined in SAP2000 using built in material models. The stress strain diagrams of these materials are provided in the references listed above. The superstructure of the bridge is a box-girder. Following the design assumptions, this element is modelled as an elastic frame using effective cross-section properties per Aviram report.<sup>37</sup>

Each span is divided in six elements in SAP2000 and the translational and rotational masses are lumped to the end nodes of these elements. A schematic description of the Finite Element Model of the bridge is given in Figures 24 to 26. Geometric (P-Delta effects) and material nonlinearity are considered in the analyses. The abutment of the bridge is modelled using nonlinear spring elements which define the response of the structure in the longitudinal, transversal, and vertical direction.<sup>37</sup> Two rubber bearings are inserted on top of each column and on the abutments below the deck. The base isolation layer modelled for the prototype bridge is that designed by Aviram.<sup>34</sup>

The design follows AASHTO specification for base isolation and the Caltrans seismic design criteria.<sup>38</sup> The first mode of vibration of the bridge is a translation of the deck in the transverse direction. The period of the first mode is 3.20 s while the period of the second mode of vibration is 2.99 s. This corresponds to a translation of the deck in the longitudinal direction. The bearings have been modelled in SAP2000 as bilinear elements. The properties of the bearings for the as new and the aged isolators are described in Table 7. The cap beam on top and on the bottom of the isolators are modelled as rigid links.

## MODELLING OF RUBBER BEARINGS FOR NRHAs INCLUDING AGING EFFECTS

### The bilinear model of hysteresis for rubber bearings

A design period of vibration of 3.0 s was selected for the base isolated model, the design equivalent damping ratio was selected to be 18% of critical. The design displacement was 560 mm. The following section describes the definition of the parameters of the bilinear model starting from the design values listed above. The same procedure could be used to derive bilinear models of base isolators from the results found in this study's experimental tests. The bilinear model of hysteresis is shown in Figure 27 in terms of base displacement,  $D$ , and horizontal force,  $F_b$ .

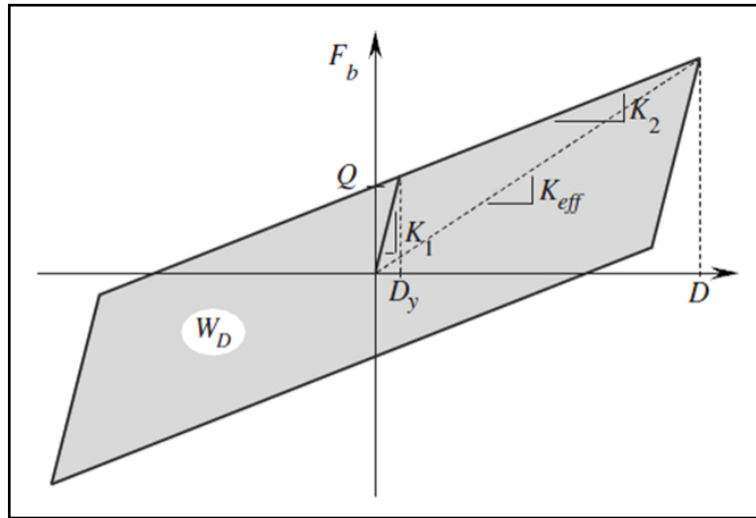


Figure 27. Bilinear Hysteretic Model and Parameters

In Figure 27,  $K_1$  is the initial stiffness,  $K_2$  is the second stiffness,  $K_{eff}$  is the effective stiffness,  $Q$  is the zero-displacement-force intercept, while  $D_y$  is the yield displacement. The following relations hold between these quantities:

$$K_1 = K_2 + \frac{Q}{D_y}, \quad K_{eff} = K_2 + \frac{Q}{D}, \quad \beta_{eff} = \frac{2Q(D - D_y)}{\pi K_{eff} D^2}$$

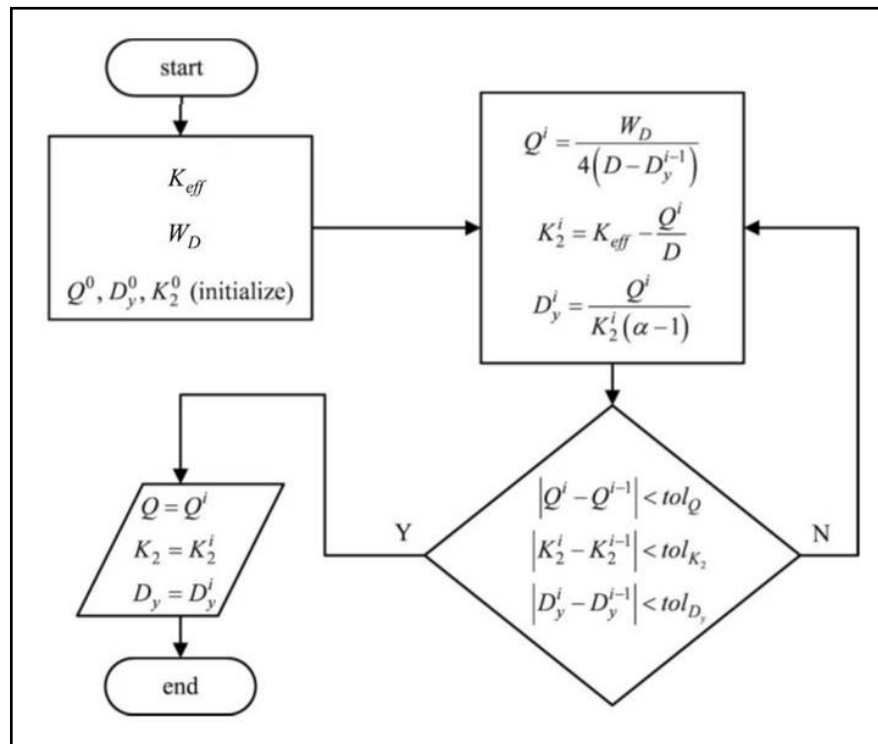
For the bilinear model, the energy dissipated in each cycle (EDC) of hysteresis is equal to:

$$W_D = 4Q(D - D_y)$$

which for an equivalent viscously damped linear oscillator with stiffness  $K_{eff}$  and damping ratio  $\beta_{eff}$  is equal to:

$$W_D = 2\pi\beta_{eff}K_{eff}D^2$$

A bilinear model can be fully defined knowing three parameters: zero-displacement-force intercept; the initial stiffness; and the second stiffness. These parameters can be determined following the iterative procedure described in the flowchart below.

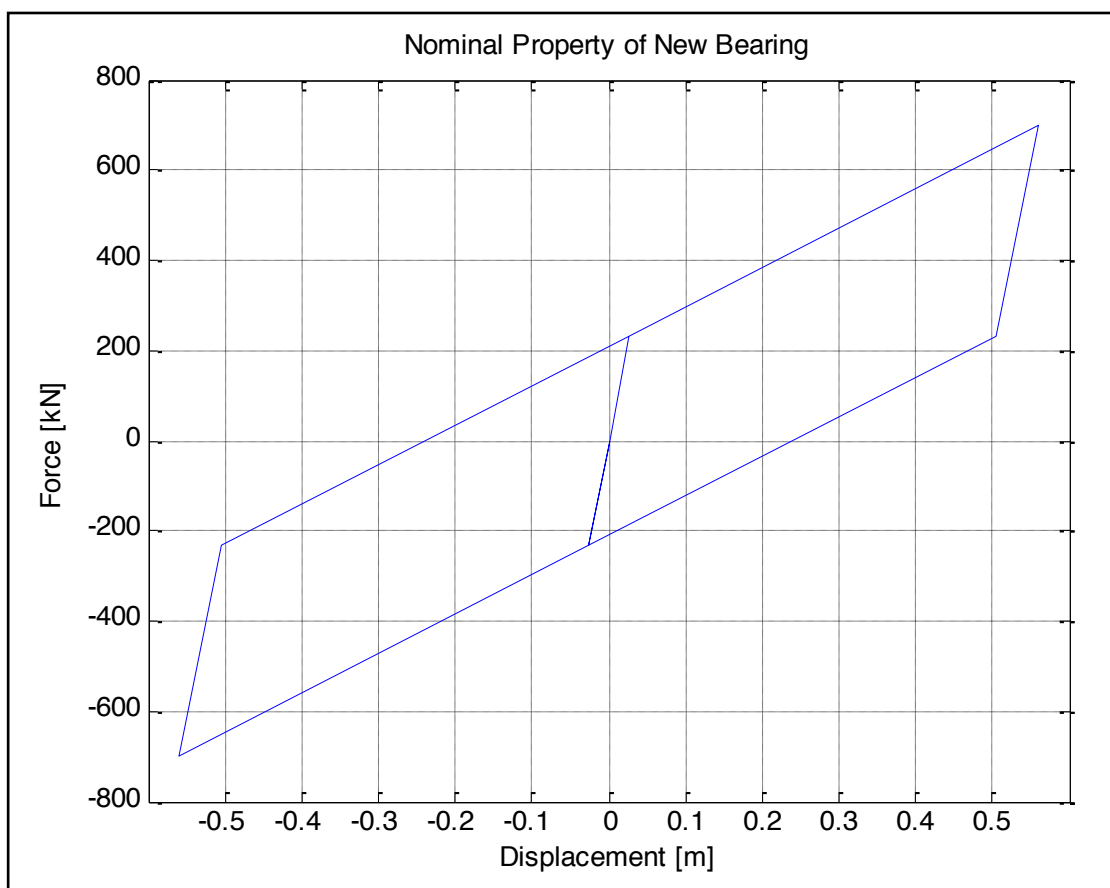


**Figure 28. Flowchart of the Iterative Procedure for the Determination of the Parameters of the Bilinear Model (Adapted from Yang Et Al.)<sup>39</sup>**

Examples of the application of this procedure are available in a research work by Yang et al.<sup>39</sup> For the bearings considered in this study, at time 0 (*i.e.*, unaged condition), the design period of isolation  $T$  is equal to 3.0 s. Knowing that the design displacement is equal to 560 mm, and the equivalent viscous damping is 18%, the EDC,  $K_1$ ,  $K_2$ ,  $K_{eff}$ , and  $Q$  were determined using the above listed formula above. The design values for the bearings considered in this study are given in Table 7. The bilinear hysteresis loop for the unaged condition is shown in Figure 29. The initial nonlinear response was assumed to be the same for the two elastomeric devices considered in this study. The aged properties of the bearings are listed in Table 7. These properties have been determined following the procedures described below.

**Table 7. Parameters of the Bilinear Model for the as New and Aged Response**

		New Bearing	Aged properties of a Neoprene Device	Aged properties of a HDRB-2
$K_{eff}$	[kN/m]	1250.7	3752.3	1500.9
T	[s]	3	3	3
$W_d$	[J]	446239	1338719	535488
$\beta_{eff}$	[%]	18.2	18.2	18.2
D	[mm]	560	560	560
Q	[kN]	209.6	628.8	251.5
$D_y$	[mm]	26.6	26.6	26.6
$K_2$	[kN/m]	875.6	2626.9	1050.8
$K_1$	[kN/m]	8756.3	26273.5	10509.4

**Figure 29. Nonlinear Response of the New Elastomeric Devices Considered in this Study**

It is worth noting that the nonlinear model considered in this study does not include any axial load-shear load interaction. Such a model is only applicable to low levels of axial loads ( $P/P_{cr} < 0.3$ ). For these magnitudes of axial loads, the shear stiffness of the bearing is not modified by the biaxial loading conditions.<sup>40</sup>

## Modelling of Aging effects on FRBs

Aging tests performed on FRBs underlined that the response of these devices can vary significantly over the service life of a bridge. In this chapter, the influence of aging on the nonlinear response of FRBs is discussed, together with the definition of models for numerical analyses capable of predicting the effects of aging on the lateral response of the bearings. As underlined by many experimental findings, the aging of elastomeric devices is significantly influenced by the bearings' manufacturing quality and material type.<sup>20, 22</sup> For conventional rubber devices, it was found that, over time, the hardening of the elastomer causes an increase in the post-elastic stiffness  $K_2$  along with the zero-displacement-force intercept,  $Q$ , of the bearings. For devices made with a low damping rubber with a shear modulus in the range of 0.5 to 1.0 MPa, it was found that the increase of the effective stiffness and equivalent viscous damping ranges between 10–20% over a span of 30 years.<sup>20</sup> In this paragraph, the model introduced by Itoh is adopted to describe the variation of the mechanical properties of aged FRBs.<sup>5, 6</sup> Starting from the results of accelerated aging tests on FRBs, the method aims to describe the variation of equivalent horizontal stiffness with time, temperature and bearing size. For a rectangular bearing, the horizontal stiffness at a time  $t$  can be determined as:

$$K_{h,eq} = \frac{G_0}{nt_r} \left[ (a - 2d^*)(b - 2d^*) + 2d^*(a + b - 4d^*) \left( 1 + \frac{\Delta G_s}{3} \right) + 4d^{*2} \left( 1 + \frac{\Delta G_s}{2} \right) \right]$$

where:

- $G_0$  is the shear modulus of the rubber at time 0;
- $a$  and  $b$  are the length and width of the bearing;
- $n$  is the number of rubber layers;
- $t_r$  is the thickness of the individual layer of rubber;
- $d^*$  is the critical depth;
- $\Delta G_s$  is the variation of shear modulus (within the critical depth) due to aging.

The critical depth,  $d^*$ , defines the volume of the bearing within which the variation of aged mechanical properties is significant. This depth can be determined with the following formula:

$$d^* = \alpha e^{\beta/T}$$

Where  $T$  is the absolute temperature,  $\alpha = 0.00012 \text{ mm}$  and  $\beta = 3.82 \times 10^{-3}$  can be determined from aging tests on rubber, as described in a work by Itoh.<sup>6</sup> Using the results of the experimental tests described in this study, for a test time  $t_{test}$  of one week, at a test temperature  $T_{test}$  of 82°C, a variation of shear stiffness up to 30% can be expected within the critical depth. The aging time  $t_{test}$  can be correlated to the real time,  $t$  using the Arrhenius methodology:

$$\ln\left(\frac{t}{t_{test}}\right) = \frac{E_a}{R} \left( \frac{1}{T} - \frac{1}{T_{test}} \right)$$

In this formula,  $R=8.314$  [J/mol K] is the gas constant,  $E_a$  is the activation energy of the rubber,  $T$  indicates the in service absolute temperature. Assuming a location with a yearly average temperature of  $17^\circ\text{C}$ , from the procedure reported above, it can be determined that for a square bearing of  $300 \times 300$  mm and a total height of the rubber of 150mm, a variation of horizontal stiffness of 10% can be expected in 50 years. A bearing of  $800 \times 800$ mm, with a total height of 254 mm would experience a variation of horizontal stiffness of only 3.3% over the same time period. It should be noted that the constants listed above were determined for steel reinforced natural rubber devices. The applicability of this procedure (and coefficients) to fiber reinforced devices should be further investigated.

### Modelling of Aging Effects for the Bearings Considered in this Study

The aging tests on neoprene FRBs described in previous chapters of this report underlined that the response of these bearings can vary significantly over the service life of a bridge. Nevertheless, experimental evidence is not sufficient to fully describe the differences in the aging characteristics of fiber and steel reinforced elastomeric bearings. For this reason, property modification factors have been adopted in this study to describe the influence of aged neoprene FRBs and conventional HDRBs with respect to their hysteretic response. The concept of using property modification factors to describe the effects of aging, temperature, wear, contamination, and scragging on the mechanical properties of isolation devices was introduced in the 1999 AASHTO Guide Specifications for Seismic Isolation Design.<sup>35</sup> The specifications provide researchers with a formula to estimate the minimum and maximum value of each quantity of interest to define the linear and the nonlinear response of bridge isolators. The methodology is applicable to elastomeric and sliding devices. A significant contribution to the definition of property modification factors for sliding devices was given by Constantinou et al.<sup>41</sup> Thompson et al.'s research describes the influence of these different phenomena on the response to rubber-based devices.<sup>42</sup> The reader can refer to Thompson et al.'s work and the AASHTO Guide Specifications for a thorough description of the use of lambda factors to bound the likely isolators' response in bridges.<sup>43</sup> In this paragraph, only the information necessary to define the effects of aging on the effective stiffness, the equivalent viscous damping ratio, the zero-displacement-force intercept and the post-yield stiffness of an elastomeric device are given. The procedure described here is based on the LRFD Seismic Analysis and Design of Bridges Reference Manual.<sup>43</sup> The coefficients listed below are based on the AASHTO Guide Specifications for LRFD Seismic Bridge Design of 2014.<sup>44</sup> The modification factors are used to estimate both minimum and maximum values for each quantity of interest. For example, based on the nominal values of  $Q_d$  and  $K_d$ , minimum and maximum values of the effective stiffness and the zero-displacement-force intercept can be computed with the following formula:

$$K_{d \max} = \lambda_{\max Kd} K_d; K_{d \min} = \lambda_{\min Kd} K_d; Q_{d \max} = \lambda_{\max Qd} Q_d; Q_{d \min} = \lambda_{\min Qd} Q_d.$$

In this formula,  $\lambda_{\min}$  is taken as one. This means that the lower bound properties are the same as their nominal values. The maximum value of the  $\lambda$ -factor ( $\lambda_{\max}$ ) for an elastomeric device can be determined with the following formula:

$$\lambda_{\max} = (\lambda_{\max,t})(\lambda_{\max,a})(\lambda_{\max,scrag})(\lambda_{\max,v})(\lambda_{\max,tr})$$

where

$\lambda_{\max,t}$  = maximum value of the  $\lambda$ -factor to consider the effects of temperature;

$\lambda_{\max,a}$  = maximum value of the  $\lambda$ -factor to consider the effects of aging;

$\lambda_{\max,scrag}$  = maximum value of the  $\lambda$ -factor to consider the effects of scragging;

$\lambda_{\max,v}$  = maximum value of the  $\lambda$ -factor to consider the effects of velocity;

$\lambda_{\max,tr}$  = maximum value of the  $\lambda$ -factor to account for the effect of travel.

The  $\lambda_{\max,t}$  and the  $\lambda_{\max,v}$  values should be determined with tests. For this study they are both taken as one. All other values, in the absence of experimental evidences, can be determined from the AASHTO Guide Specifications.  $\lambda_{\max,t}$  is the value of the  $\lambda$ -factor to consider the effects of temperature. In this study, a minimum temperature for design of 21°C is assumed ( $\lambda_{\max,t}=1$ ). The maximum value of the  $\lambda$ -factor to consider the effects of aging,  $\lambda_{\max,a}$ , was based on values listed in Table 8. Two cases were considered to describe the aging of High Damping Rubber Bearings with small differences (<25%) between scragged and unscragged properties (HDRB-2,  $\lambda_{\max,a} = 1.2$ ), and the aging of neoprene bearings ( $\lambda_{\max,a} = 3.0$ ).

**Table 8. Maximum Values of Aging  $\lambda$ -Factors for Elastomeric Isolators<sup>44</sup>**

Material	$K_d$	$Q_d$
Low Damping Natural Rubber (LDRB)	1.1	1.1
High Damping Rubber with large differences (>25%) between scragged and unscragged properties (HDRB-1)	1.3	1.3
High Damping Rubber with small differences (<25%) between scragged and unscragged properties (HDRB-2)	1.2	1.2

The effects of scragging on the response of the bearings are not considered in this study. The effects of the modification factors on the nonlinear response of a rubber-based device are shown in Figure 30.

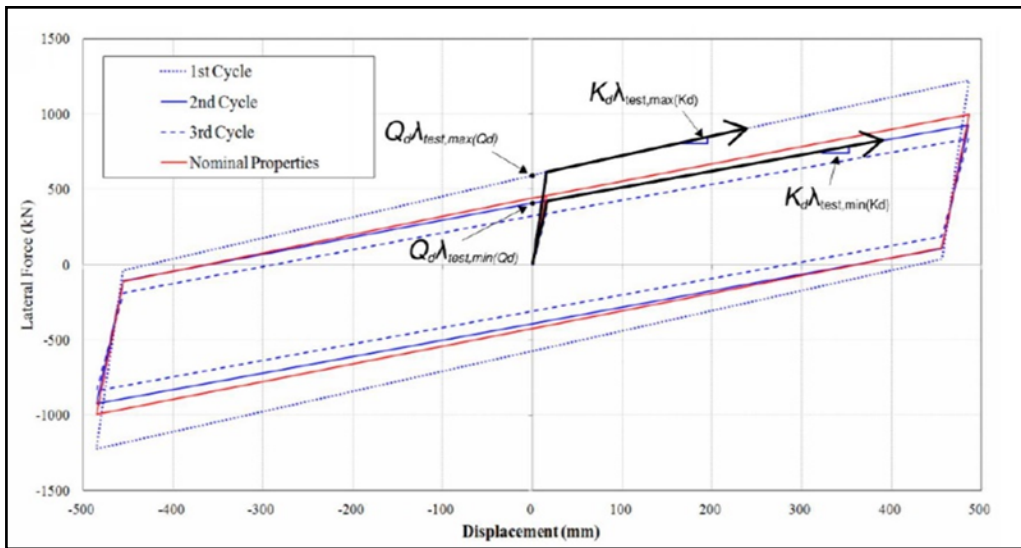


**Figure 30. Effects of the Modification Factors on the Nonlinear Repose of a Base Isolation Device<sup>44</sup>**

Following the procedure described above, the aged response of the bearings has been determined. The upper and lower bound force–displacement response is plotted for aged HDRB-2 and neoprene bearings in Figure 31.

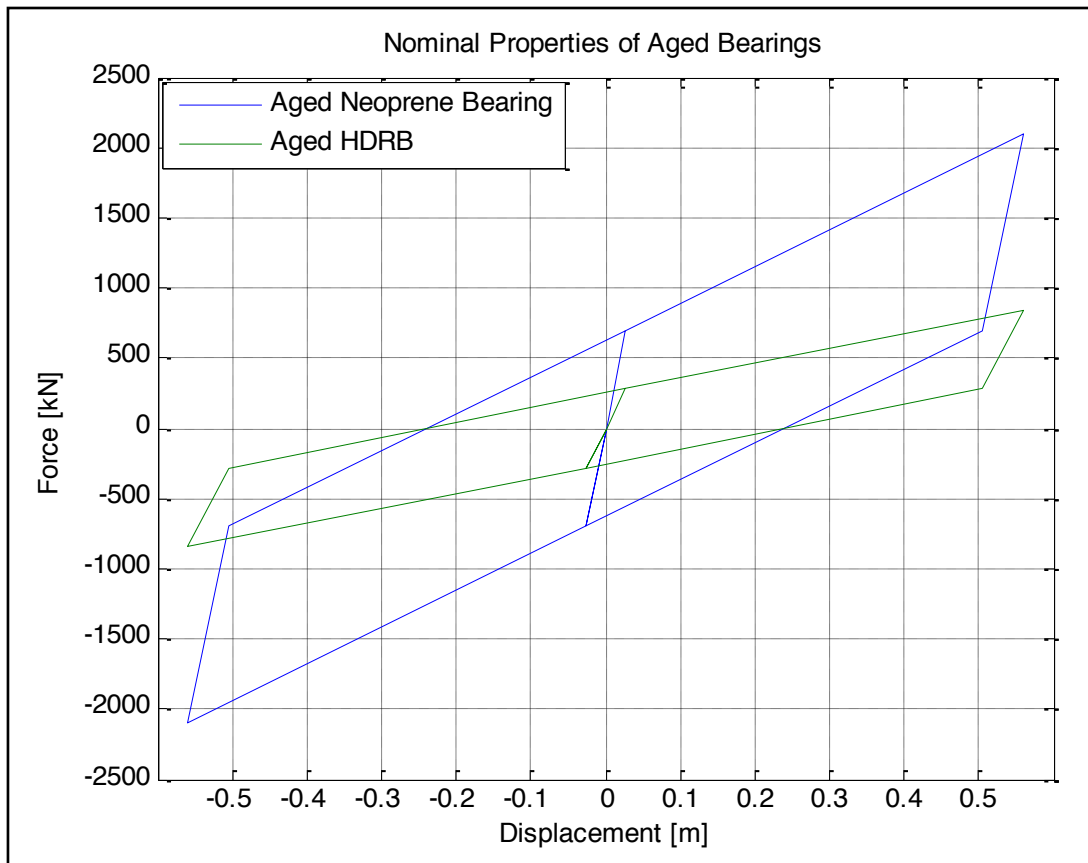


**Figure 31. Nonlinear Response of Aged Elastomeric Devices Considered in this Study**

## **GROUND MOTION SELECTION**

Two sets of uniform ground motions were applied at the base of the bridge with the characteristics of each set shown in Table 9. The two sets include the Far-Field Record set (this set includes 21 events recorded at sites located at a distance greater or equal to 10 km) and 28 Near-Field Records described in FEMA P695/June 2009.<sup>45</sup> The Near-Field record set includes records with strong pulses, referred to as the “NF-Pulse.” This selection, furthermore, covers a wide range of magnitude, epicentral distances and fault mechanisms. The events were used in this study as representative of very strong ground motions corresponding to the MCE motion in high seismic regions.

**Table 9. Summary of the Events Selected for the Analyses**

Recorded Motions												
Id No.	M	Year	Name	Recording Station	Site Data	Fault	Epicentral	Record	Files Names - Horizontal Records			
				Name	NEHRP class	Type	Distance	Seq. No.	Component 1	Component 2	PGA max	PGV max
[-]	[-]	[-]	[-]	[-]	[-]	[-]	[km]	[-]	[-]	[-]	[g]	[cm/s]
1	6.7	1994	Northridge	Beverly Hills - Mulhol	D	Thrust	13.3	953	NORTHR/MUL009	NORTHR/MUL279	0.52	63
2	6.7	1994	Northridge	Canyon Country-WLC	D	Thrust	26.5	960	NORTHR/LOS000	NORTHR/LOS270	0.48	45
3	7.1	1999	Duzce, Turkey	Bolu	D	Strike-slip	41.3	1602	DUZCE/BOL000	DUZCE/BOL090	0.82	62
4	7.1	1999	Hector Mine	Hector	D	Strike-slip	26.5	1787	HECTOR/HEC000	HECTOR/HEC090	0.34	42
5	6.5	1979	Imperial Valley	Delta	D	Strike-slip	33.7	169	IMPVALL/H-DLT262	IMPVALL/H-DLT352	0.35	33
6	6.5	1979	Imperial Valley	El Centro Array #11	D	Strike-slip	29.4	174	IMPVALL/H-E11140	IMPVALL/H-E11230	0.38	42
7	6.9	1995	Kobe, Japan	Nishi-Akashi	D	Strike-slip	8.7	1111	KOBE/NIS000	KOBE/NIS090	0.51	37
8	6.9	1995	Kobe, Japan	Shin-Osaka	D	Strike-slip	46.0	1116	KOBE/SHI000	KOBE/SHI090	0.24	38
9	7.5	1999	Kocaeli, Turkey	Duzce	D	Strike-slip	98.2	1158	KOCAELI/DZC180	KOCAELI/DZC270	0.36	59
10	7.5	1999	Kocaeli, Turkey	Arcelik	D	Strike-slip	53.7	1148	KOCAELI/ARC000	KOCAELI/ARC090	0.22	40
11	7.3	1992	Landers	Yermo Fire Station	D	Strike-slip	86.0	900	LANDERS/YER270	LANDERS/YER360	0.24	52
12	7.3	1992	Landers	Coolwater	D	Strike-slip	82.1	848	LANDERS/CLW-LN	LANDERS/CLW-TR	0.42	42
13	6.9	1989	Loma Prieta	Capitola	D	Strike-slip	9.8	752	LOMAP/CAP000	LOMAP/CAP090	0.53	35
14	6.9	1989	Loma Prieta	Gilroy Array #3	D	Strike-slip	31.4	767	LOMAP/G03000	LOMAP/G03090	0.56	45
15	7.4	1990	Manjil, Iran	Abbar	D	Strike-slip	40.4	1633	MANJIL/ABBAR--L	MANJIL/ABBAR--T	0.51	54
16	6.5	1987	Superstition Hills	El Centro Imp. Co.	D	Strike-slip	35.8	721	SUPERST/B-ICC000	SUPERST/B-ICC090	0.36	46
17	6.5	1987	Superstition Hills	Poe Road (temp)	D	Strike-slip	11.2	725	SUPERST/B-POE270	SUPERST/B-POE360	0.45	36
18	7.6	1999	Chi-Chi, Taiwan	CHY101	D	Thrust	32.0	1244	CHICHI/CHY101-E	CHICHI/CHY101-N	0.44	115
19	7.6	1999	Chi-Chi, Taiwan	TCU045	D	Thrust	77.5	1485	CHICHI/TCU045-E	CHICHI/TCU045-N	0.51	39
20	6.6	1971	San Fernando	LA - Hollywood Stor	D	Thrust	39.5	68	SFERN/PEL090	SFERN/PEL180	0.21	19
21	6.5	1976	Friuli, Italy	Tolmezzo	D	Thrust	20.2	125	FRIULI/A-TMZ000	FRIULI/A-TMZ270	0.35	31

**Table 9, continued**

Recorded Motions													
Id No.	M	Year	Name	Recording Station	Site Data	Fault	Epicentral	Record	Files Names - Horizontal Records			PGA max	PGV max
				Name	NEHRP class	Type	Distance	Seq. No.	Component 1	Component 2			
[-]	[-]	[-]	[-]	[-]	[-]	[-]	[km]	[-]	[-]	[-]	[g]	[cm/s]	
Pulse													
22	6.5	1979	Imperial Valley-06	El Centro Array #6	D	Strike-slip	27.5	181	IMPVALL/H-E06_233	IMPVALL/H-E06_323	0.44	111.9	
23	6.5	1979	Imperial Valley-06	El Centro Array #7	D	Strike-slip	27.6	182	IMPVALL/H-E07_233	IMPVALL/H-E07_323	0.46	108.9	
24	6.9	1980	Irpinia, Italy-01	Sturno	B	Normal	30.4	292	ITALY/A-STU_223	ITALY/A-STU_313	0.31	45.5	
25	6.5	1987	Superstition Hills-02	Parachute Test Site	D	Strike-slip	16.0	723	SUPERST/B-PTS_037	SUPERST/B-PTS_127	0.42	106.8	
26	6.9	1989	Loma Prieta	Saratoga - Aloha	C	Strike-slip	27.2	802	LOMAP/STG_038	LOMAP/STG_128	0.38	55.6	
27	6.7	1992	Erzican, Turkey	Erzincan	D	Strike-slip	9.0	821	ERZIKAN/ERZ_032	ERZIKAN/ERZ_122	0.49	95.5	
28	7.0	1992	Cape Mendocino	Petrolia	C	Thrust	4.5	828	CAPEMEND/PET_260	CAPEMEND/PET_350	0.63	82.1	
29	7.3	1992	Landers	Lucerne	C	Strike-slip	44.0	879	LANDERS/LCN_239	LANDERS/LCN_329	0.79	140.3	
30	6.7	1994	Northridge-01	Rinaldi Receiving Sta	D	Thrust	10.9	10630	NORTHR/RRS_032	NORTHR/RRS_122	0.87	167.3	
31	6.7	1994	Northridge-01	Sylmar - Olive View	C	Thrust	16.8	1086	NORTHR/SYL_032	NORTHR/SYL_122	0.73	122.8	
32	7.5	1999	Kocaeli, Turkey	Izmit	B	Strike-slip	5.3	1165	KOCAELI/IZT_180	KOCAELI/IZT_270	0.22	29.8	
33	7.6	1999	Chi-Chi, Taiwan	TCU065	D	Thrust	26.7	1503	CHICHI/TCU065_272	CHICHI/TCU065_002	0.82	127.7	
34	7.6	1999	Chi-Chi, Taiwan	TCU102	C	Thrust	45.6	1529	CHICHI/TCU102_278	CHICHI/TCU102_008	0.29	106.6	
35	7.1	1999	Duzce, Turkey	Duzce	D	Strike-slip	1.6	1605	DUZCE/DZC_172	DUZCE/DZC_262	0.52	79.3	
No Pulse													
36	6.8	6.8	Gazli, USSR	Karakyr	C	Thrust	12.8	126	GAZLI/GAZ_177	GAZLI/GAZ_267	0.71	71.2	
37	6.5	1979	Imperial Valley-06	Bonds Corner	D	Strike-slip	6.2	160	IMPVALL/H-BCR_233	IMPVALL/H-BCR_32	0.76	44.3	
38	6.5	1979	Imperial Valley-06	Chihuahua	D	Strike-slip	18.9	165	IMPVALL/H-CHI_233	IMPVALL/H-CHI_323	0.28	30.5	

**Table 9, continued**

Recorded Motions												
Id No.	M	Year	Name	Recording Station	Site Data	Fault	Epicentral	Record	Files Names - Horizontal Records			
				Name	NEHRP class	Type	Distance	Seq. No.	Component 1	Component 2	PGA max	PGV max
[-]	[-]	[-]	[-]	[-]	[-]	[-]	[km]	[-]	[-]	[-]	[g]	[cm/s]
39	6.8	1985	Nahanni, Canada	Site 1	C	Thrust	6.8	495	NAHANNI/S1_070	NAHANNI/S1_160	1.18	43.9
40	6.8	1985	Nahanni, Canada	Site 2	C	Thrust	6.5	496	NAHANNI/S2_070	NAHANNI/S2_160	0.45	34.7
41	6.9	1989	Loma Prieta	BRAN	C	Strike-slip	9.0	741	LOMAP/BRN_038	LOMAP/BRN_128	0.64	55.9
42	6.9	1989	Loma Prieta	Corralitos	C	Strike-slip	7.2	753	LOMAP/CLS_038	LOMAP/CLS_128	0.51	45.5
43	7.0	1992	Cape Mendocino	Cape Mendocino	C	Thrust	10.4	825	CAPEMEND/CPM_260	CAPEMEND/CPM_350	1.43	119.5
44	6.7	1994	Northridge-01	LA - Sepulveda VA	C	Thrust	8.5	1004	NORTHTR/0637_032	NORTHTR/0637_122	0.73	70.1
45	6.7	1994	Northridge-01	Northridge - Saticoy	D	Thrust	3.4	1048	NORTHTR/STC_032	NORTHTR/STC_122	0.42	53.2
46	7.5	1999	Kocaeli, Turkey	Yarimca	D	Strike-slip	19.3	1176	KOCAELI/YPT_180	KOCAELI/YPT_270	0.31	73
47	7.6	1999	Chi-Chi, Taiwan	TCU067	C	Thrust	28.7	1504	CHICHI/TCU067_285	CHICHI/TCU067_015	0.56	91.8
48	7.6	1999	Chi-Chi, Taiwan	TCU084	C	Thrust	8.9	1517	CHICHI/TCU084_271	CHICHI/TCU084_001	1.16	115.1
49	7.9	2002	Denali, Alaska	TAPS Pump Sta. #10	C	Strike-slip	7.0	2114	DENALI/ps10_199	DENALI/ps10_289	0.33	126.4

The magnitude-distance of the two sets of events is shown in Figure 33.

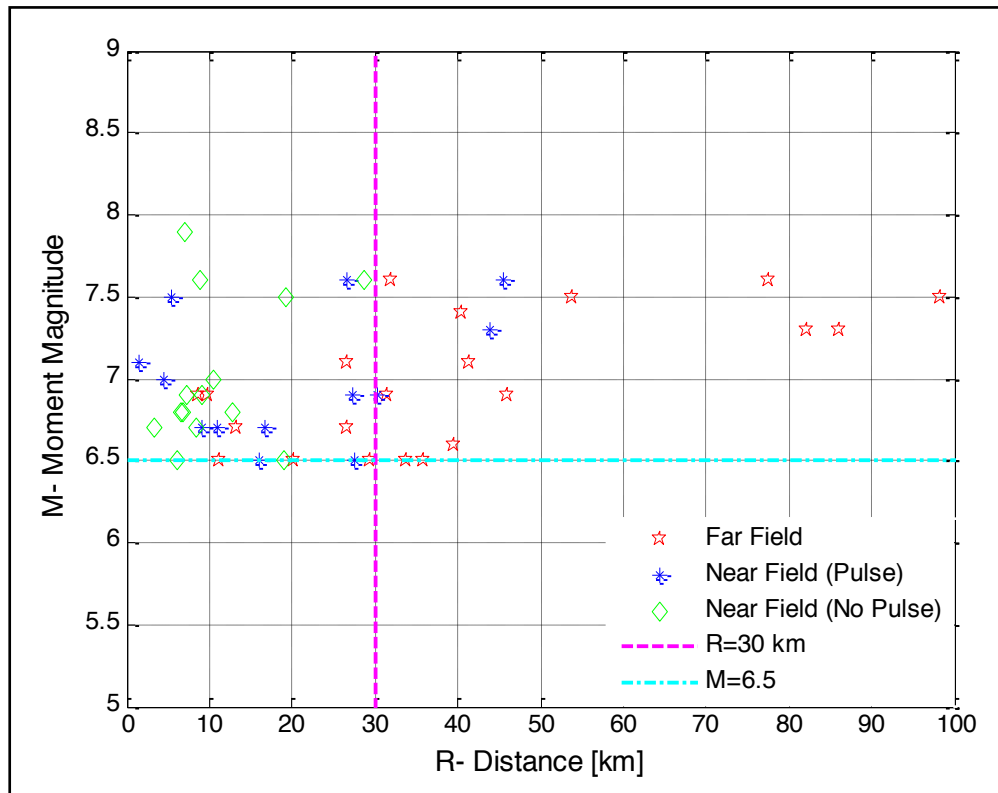


**Figure 32. Epicentral Distance vs. Magnitude of the Events Selected for this Study**

The scaling of ground motions to a given period range is not suited for bridges. The method was developed for building structures with well-spaced modes of vibration. For this reason, uniform scale factors equal to 3.0 and 1.5 and were used for the Far-Field set and the Near-Field Set respectively. The scaling factors were selected to capture the nonlinear response of the structure under large seismic events.

## DEFINITION OF THE INTENSITY MEASURES (IMS) TO BE USED FOR THE ANALYSIS OF THE STRUCTURAL RESPONSE

As a result of the analyses, different Engineering Demand Parameter (EDP) were determined including peak column ductility, peak base shear, peak displacement of the isolator, the maximum (tension) and minimum (compression) axial load on the bearing, and peak vertical acceleration of the deck. Figure 34 shows the elements of the structural model for which the EDPs have been determined.

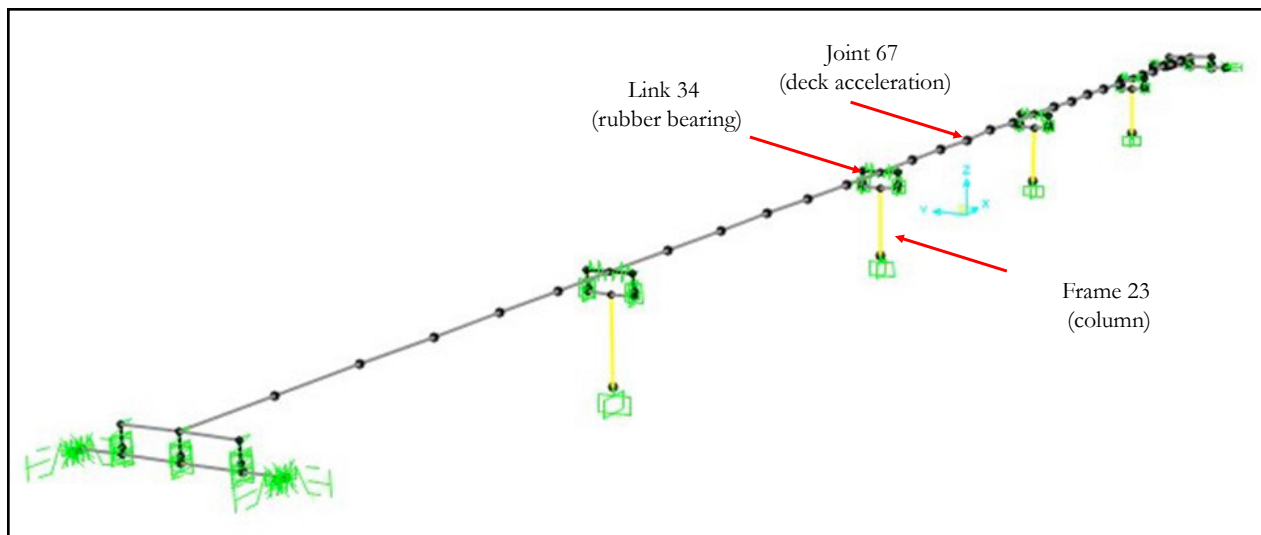


**Figure 33. Elements for which the EDPs have been Determined**

EDPs were further plotted against different period-independent Intensity Measures, include: the Peak Ground Acceleration (PGA); the Peak Ground Velocity (PGV); the Peak Ground Velocity PEER; the Peak Ground Displacement (PGD); the Acceleration RMS; the Velocity RMS; the Displacement RMS; the Arias Intensity; the Characteristic Intensity; the Specific Energy Density; the Cumulative Absolute Velocity; the Acceleration Spectrum Intensity; the Velocity Spectrum Intensity; the Housner Intensity; the Effective Design Acceleration; the Max Incremental Velocity; and the Damage Index. For each record, the PGA, PGV, and PGD were obtained as the SRSS combination of the peak ground values of the two orthogonal horizontal components of the record. A natural logarithmic regression was then used to relate the EDPs to the period-independent IMs. From the regression analysis, the coefficient of determination,  $R^2$ , was then computed. This can be interpreted as a measure of how well the observed outcomes are fitted by the logarithmic regression.<sup>46</sup> From the study of the coefficients of determination, the PGV was selected for the Far-Field and the NF-no pulse record set. The PGA was selected for the NF-pulse record set.

## RESULTS

A comparison of the performance of the fixed base model versus the response of the base isolated one has not been discussed in this work. The reader interested in such a comparison can find a detailed analysis of the response of base isolated bridges against that of fixed base bridges in Aviram. The author found that base isolated models have a higher performance than fixed base bridges under seismic excitations of different intensities. Aviram concluded that significant reductions in force and displacement demands can be obtained at the substructure when the bridge is base isolated.

This result was found to be independent of the base isolation system in use. Moreover, base isolated bridges lead to trivial post-earthquake repair efforts. The adoption of these passive protection devices allowed for continuous operation of the structure and negligible indirect costs resulting from down time.<sup>34</sup> This is because the majority of base isolated bridges are designed to ensure elastic behavior of the columns and the deck.

The model considered in this study is not representative of this type of behavior in the sense that, under large seismic excitations, the columns of the tested structure undergo a nonlinear deformation. This model was selected for this study to assess the influence of the aging of rubber bearings on the nonlinear response of the bridge's columns, due to large seismic shakings. The force and deformation demands on key components of the bridge have been compared when the elastomeric device's new and aged response was included in a 3D model of the structure.

Results of NRHAs performed in SAP 2000 are plotted against period independent intensity measures (IMs) from Figures 35–46. The data has been fitted using a power trendline. Because of the many outliers, these regression lines do not fit the data well. For this reason, the results of this study can only provide readers with general information on the tendency of the response of the bridge. The trendlines are not exact relations between the IMs and the EDPs. Nevertheless, results of this study offer an insight into the effects of aging of the isolators on the seismic response of the structure.

According to Figure 35, the deformation demand on the bearings reduces significantly with the aging of the devices. This effect is more pronounced for neoprene bearings than for HDNRBs. The displacement demand on the isolators is reduced because the force at zero displacement,  $Q$ , and the second stiffness of an aged device are much larger than those of a new bearing. As aged bearings are stiffer than new isolators, the efficiency of base isolation reduces with time. The increase in force demand on the column of the bridge is more pronounced for neoprene devices than for HDNRBs (Figure 38).

This modification of the structural response is evident under ground motions of different intensities. Figure 37 shows that the aging of the isolators has a negligible effect on the vertical acceleration of the deck. This is true for all intensity levels and for NF-pulse motions as well (see Figure 43). Under all the seismic events, the bearings of the bridge remain compressed. No tensile loads were generated by the dynamic excitation. The aging of the elastomeric devices seems to have a negligible effect on the axial load on the bearings (see Figures 36 and 42). Moreover, the column ductility demand increases with the aging of the elastomer. This effect is more pronounced under field events than under field ones (see Figures 40 and 46). As is clear in Figure 39, results of the analyses show a similar trend for the top column rotation.

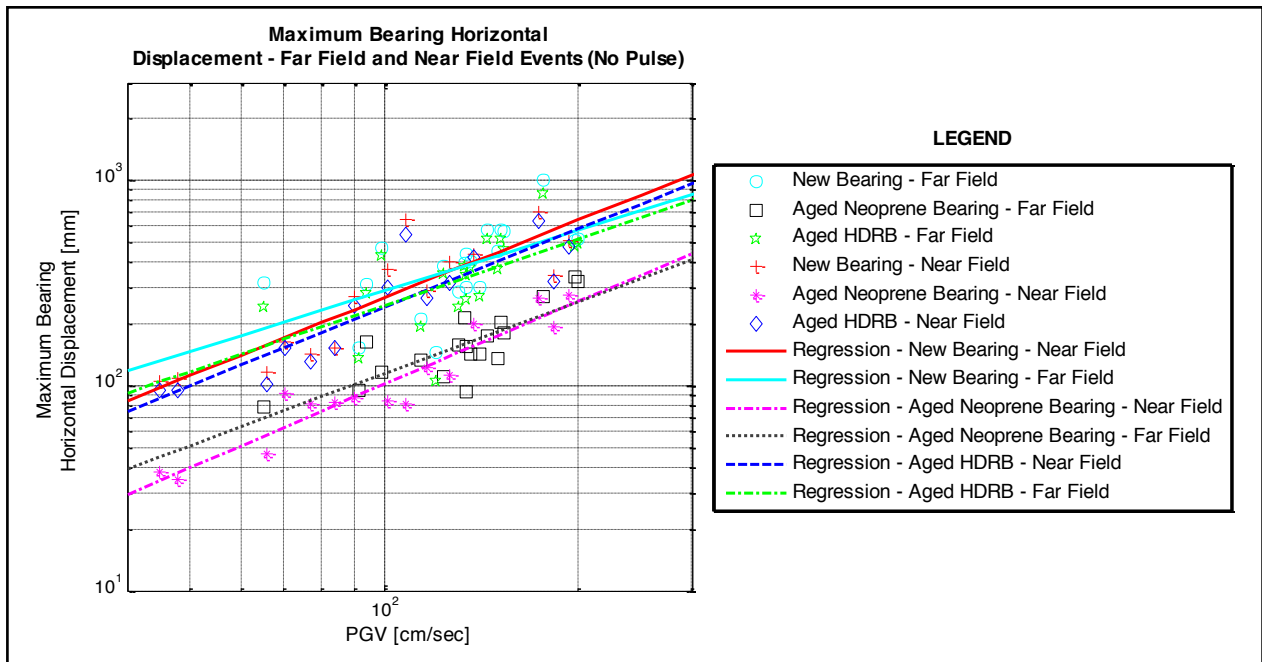


**Figure 34. Peak Horizontal Displacement of the Isolator vs. PGV**

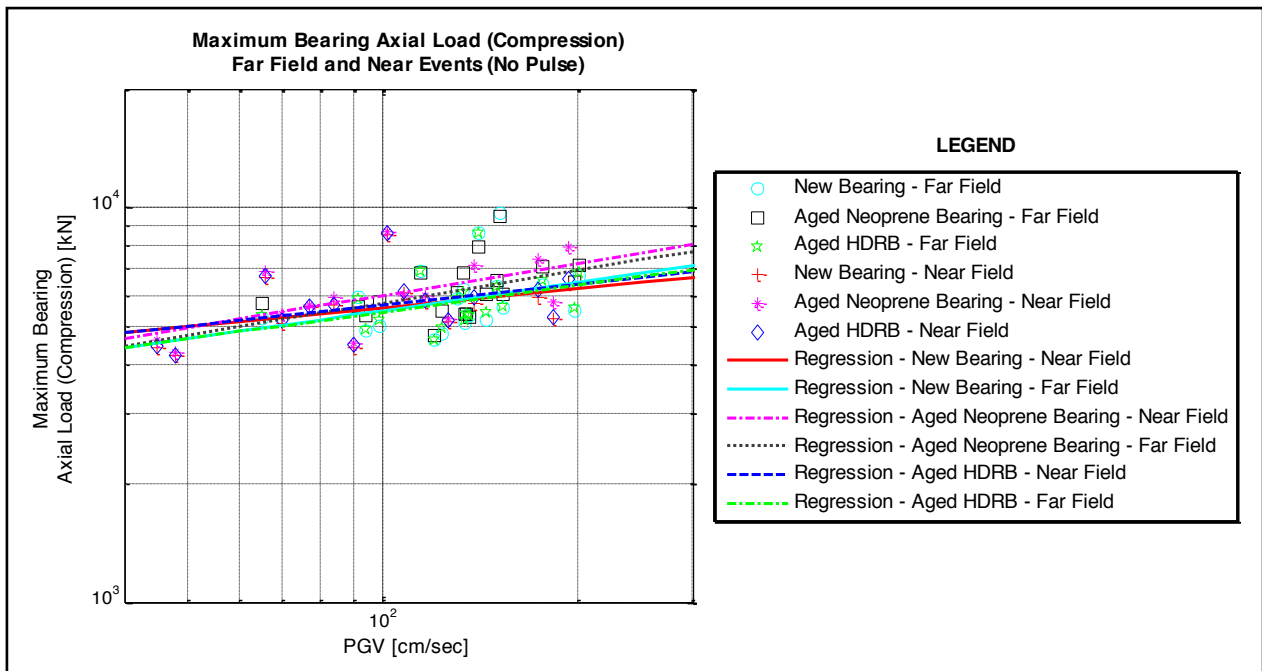


**Figure 35. Peak Axial Load on the Bearing vs. PGV**

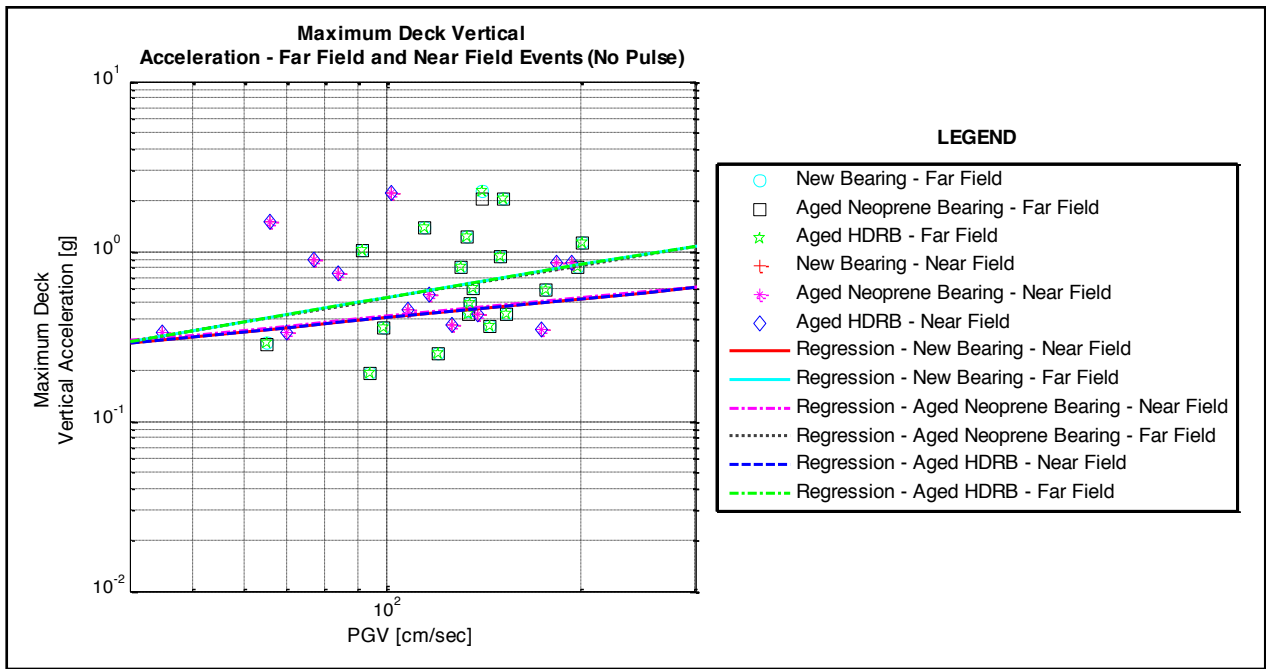


**Figure 36. Peak Vertical Acceleration of the Deck vs. PGV**

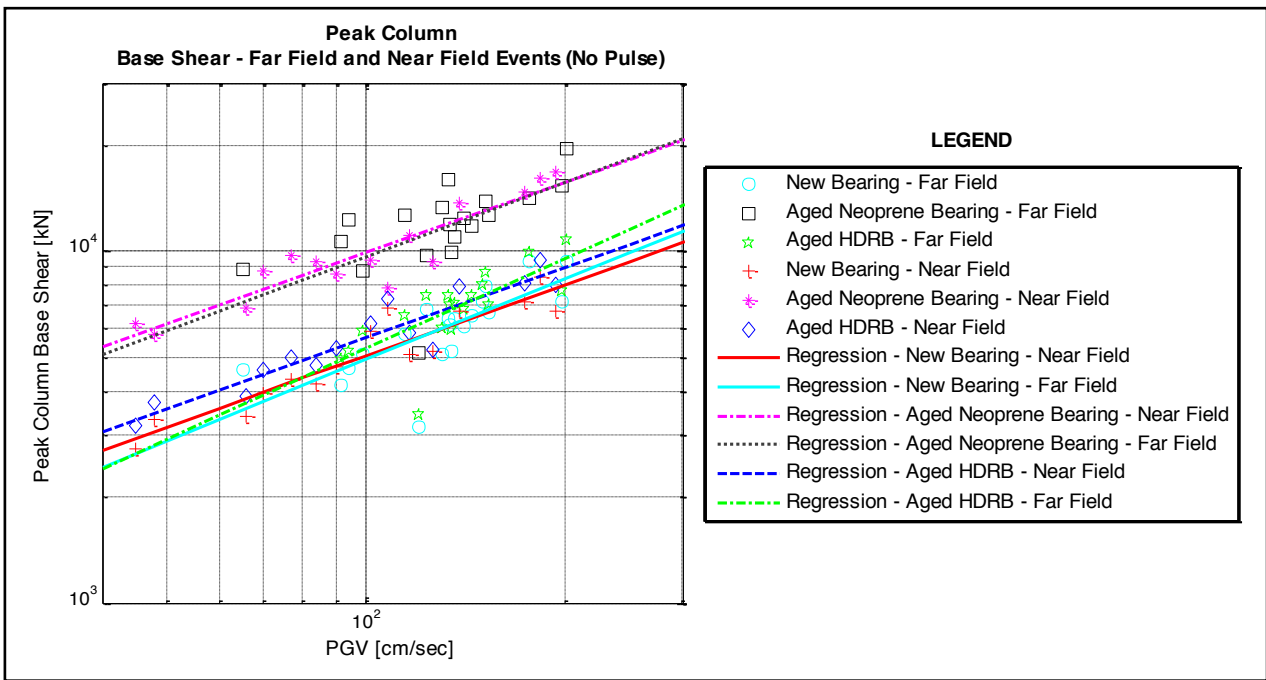


**Figure 37. Peak column Base Shear vs. PGV**

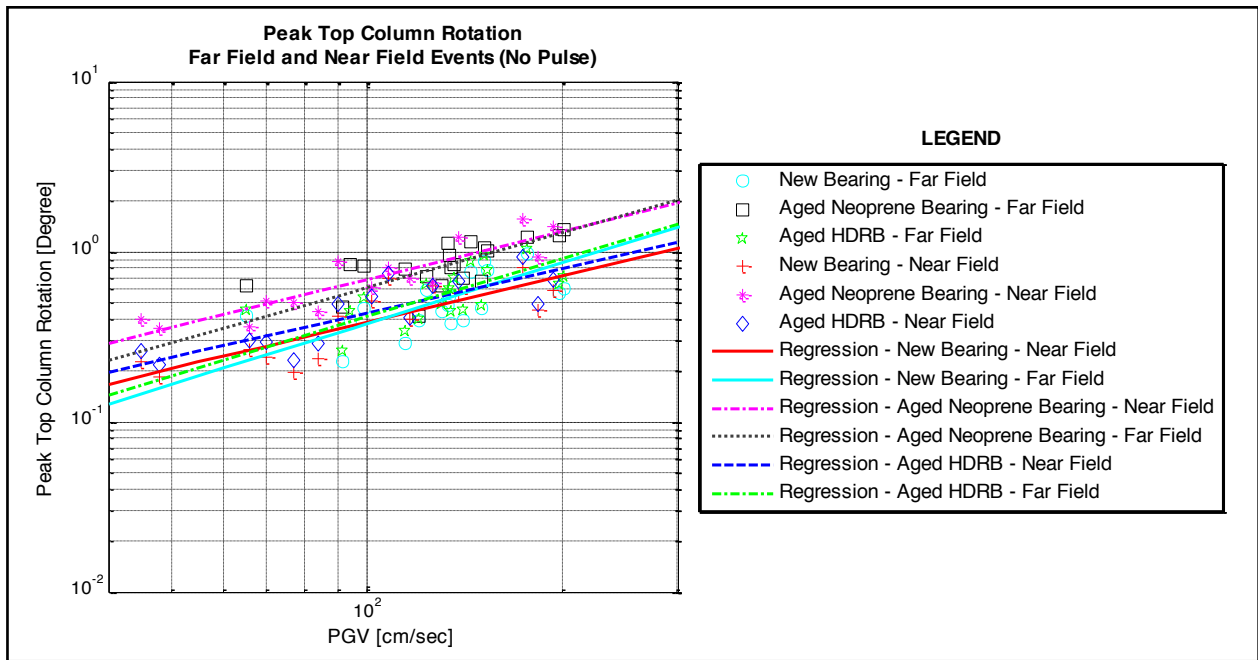


Figure 38. Peak Top Column Rotation vs. PGV

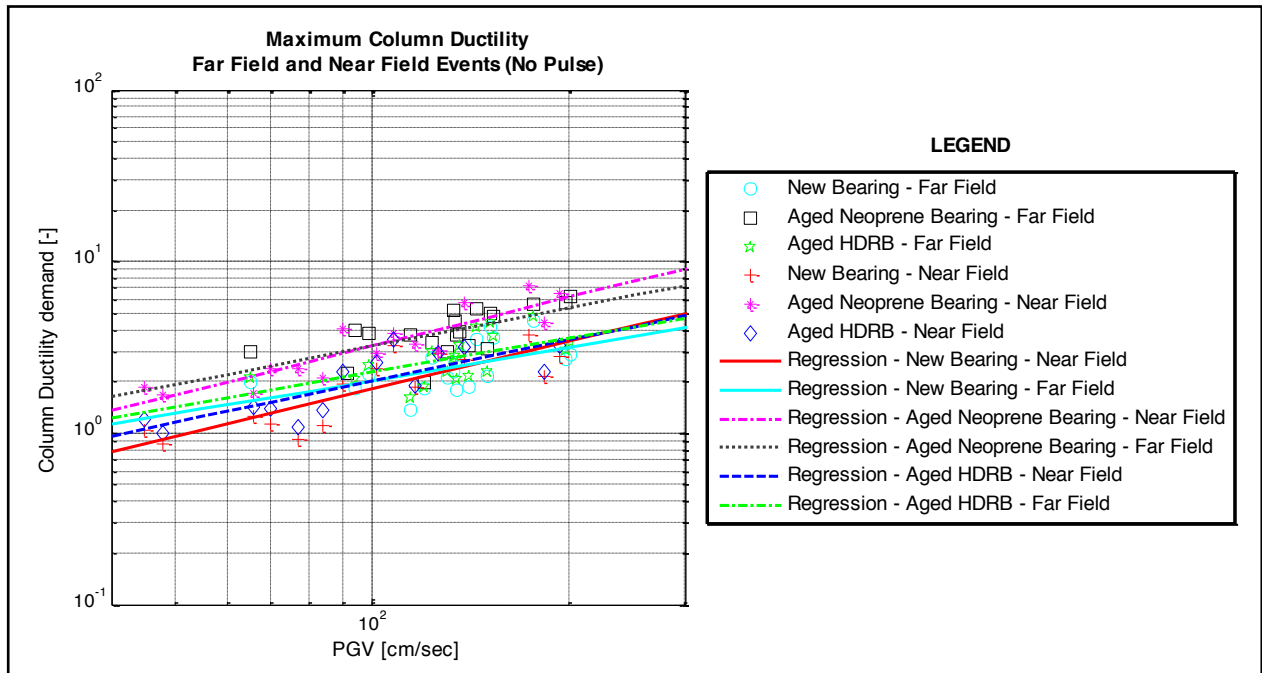
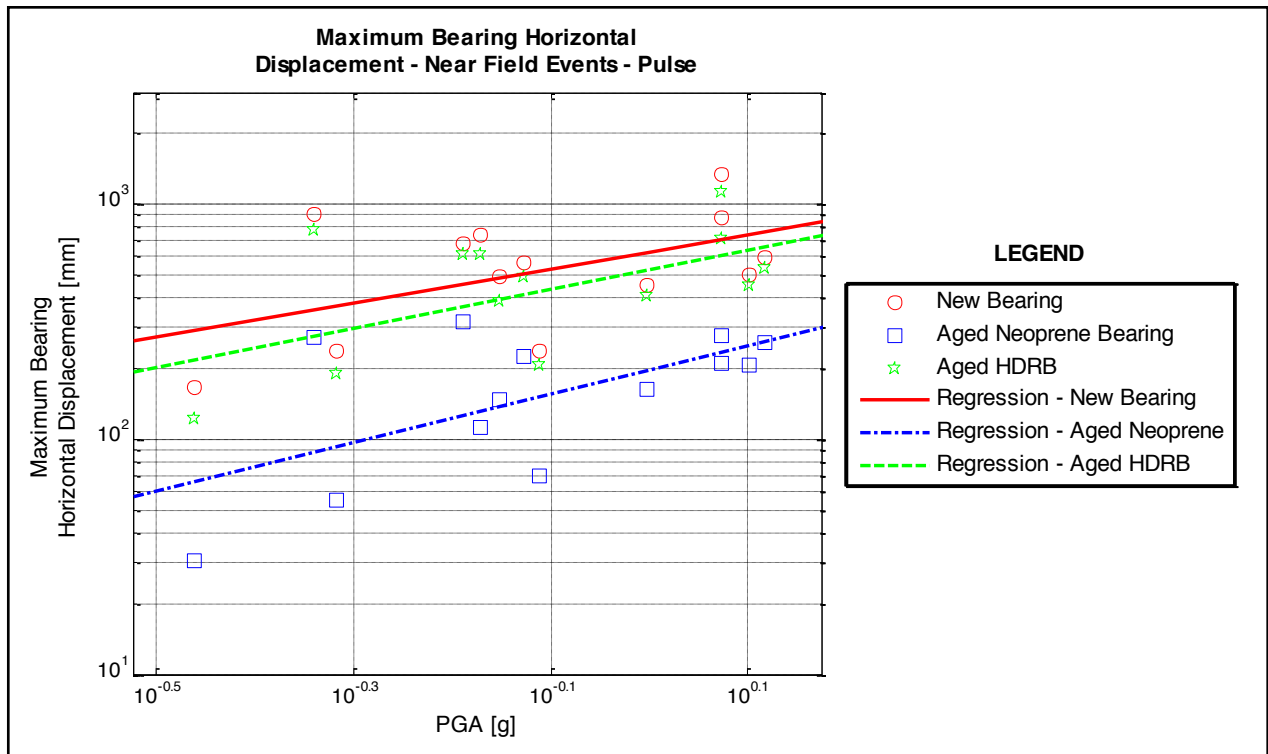
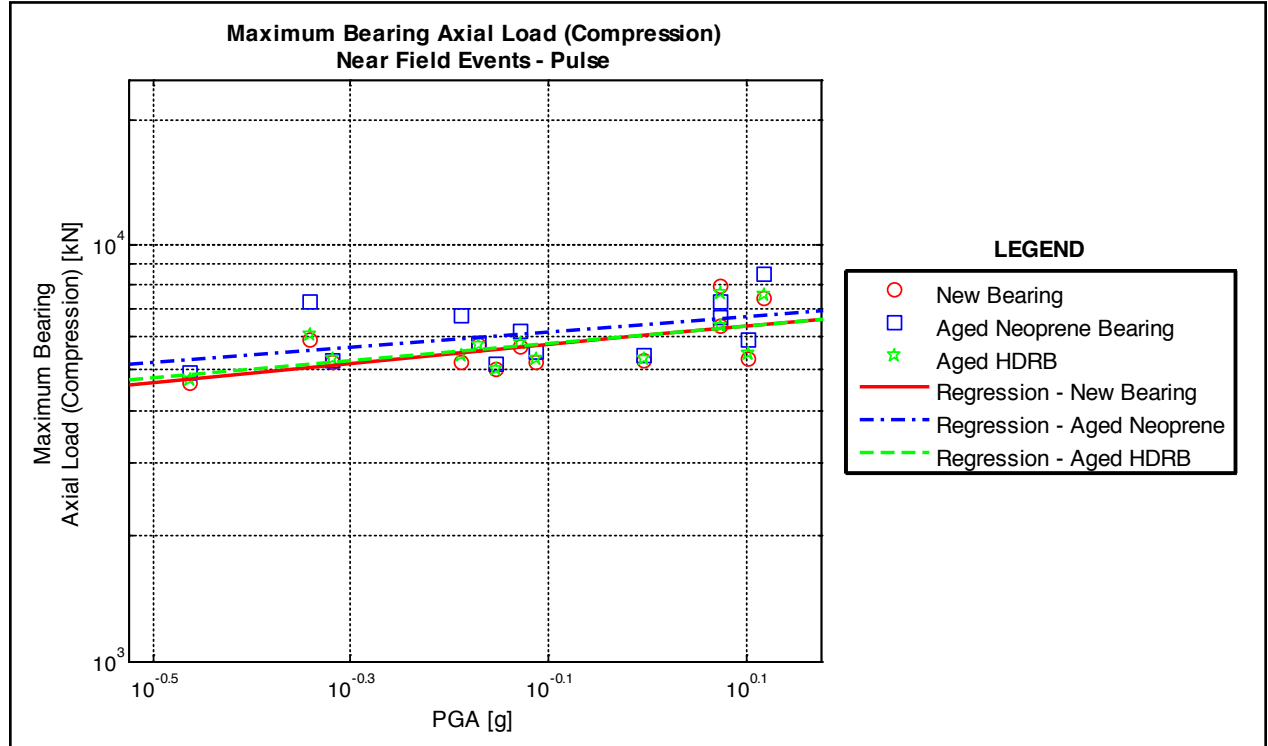


Figure 39. Peak Column Ductility Demand vs. PGV



**Figure 40. Peak Horizontal Displacement of the Isolator vs. PGA (NF-pulse record set)**



**Figure 41. Maximum Axial Load on the Bearing vs. PGA (NF-pulse record set)**

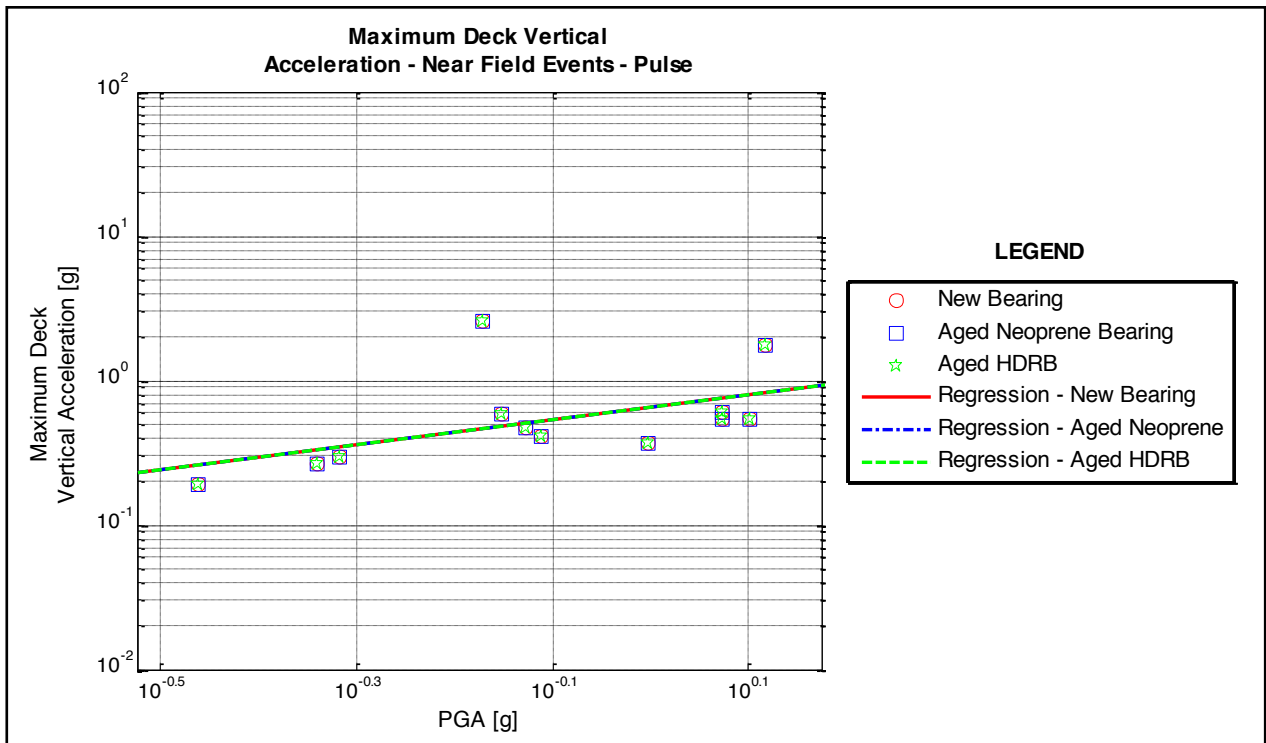


Figure 42. Peak Vertical Acceleration of the Deck vs. PGA (NF-pulse record set)

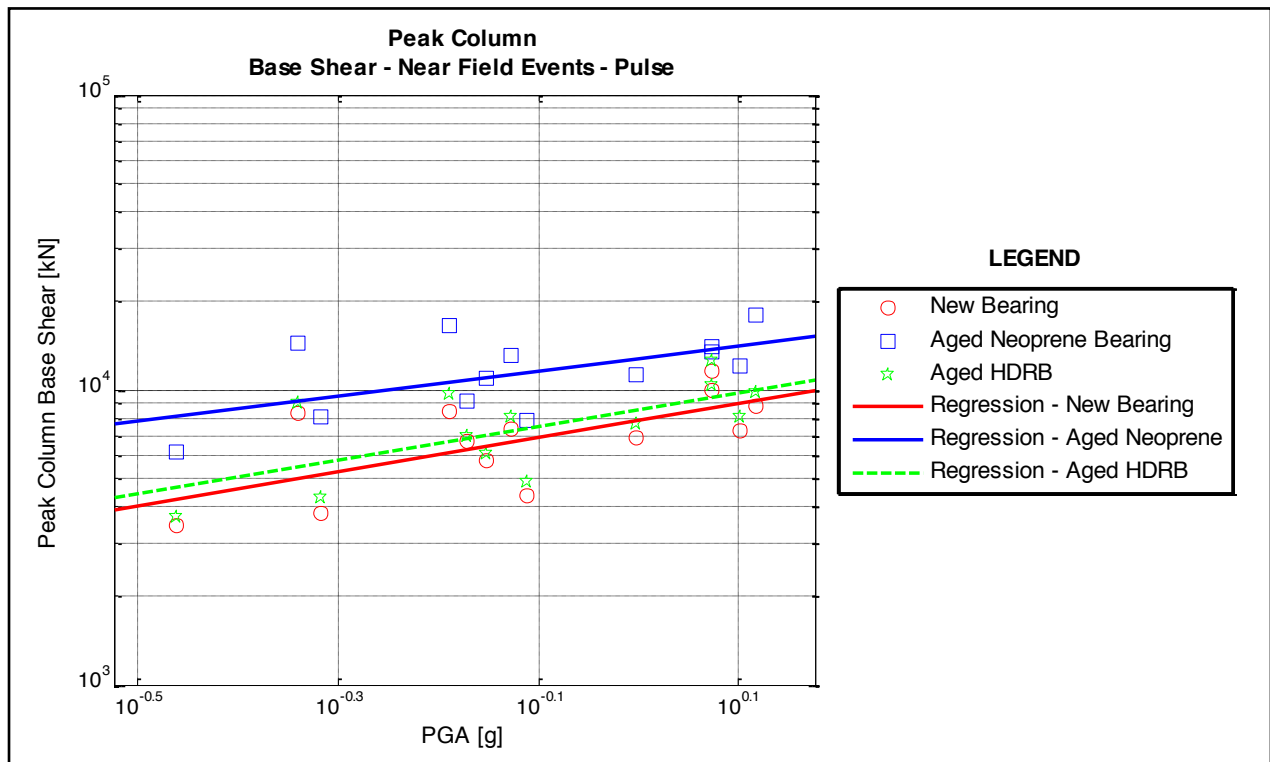


Figure 43. Peak Column Base Shear vs. PGA (NF-pulse record set)

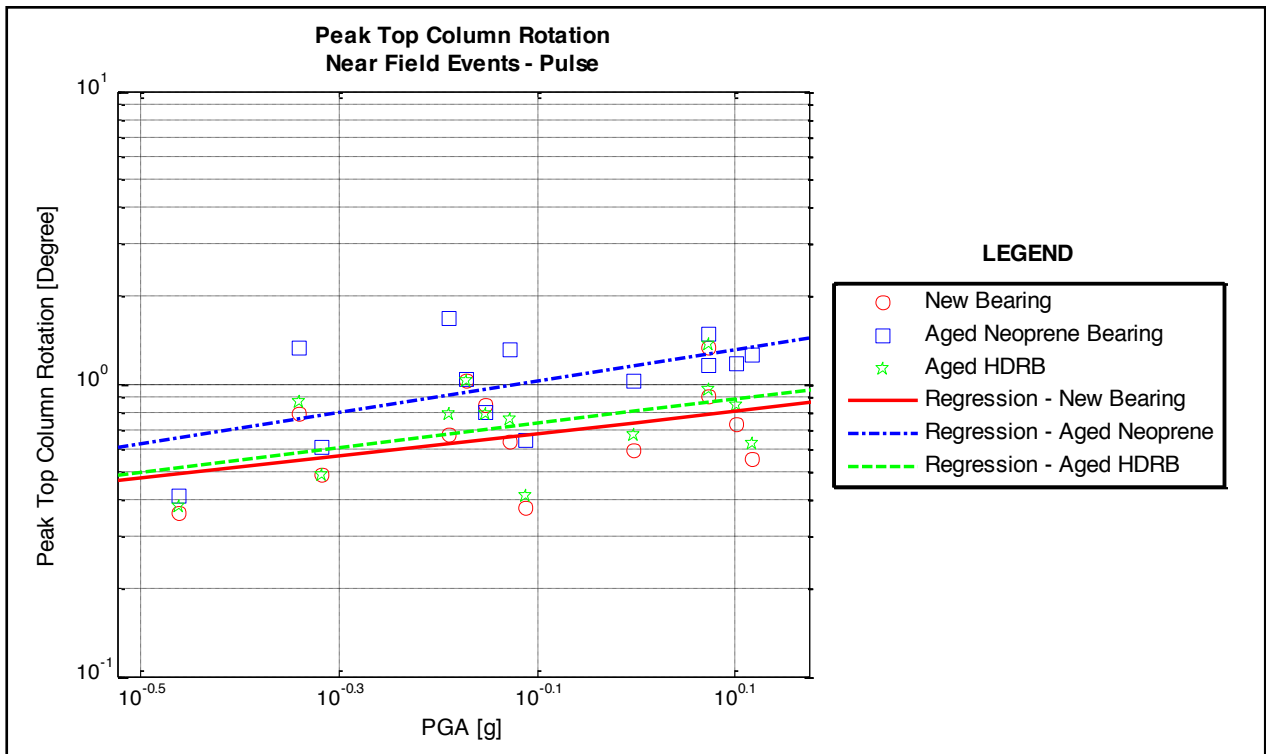


Figure 44. Peak Top Column Rotation vs. PGA (NF-pulse record set)

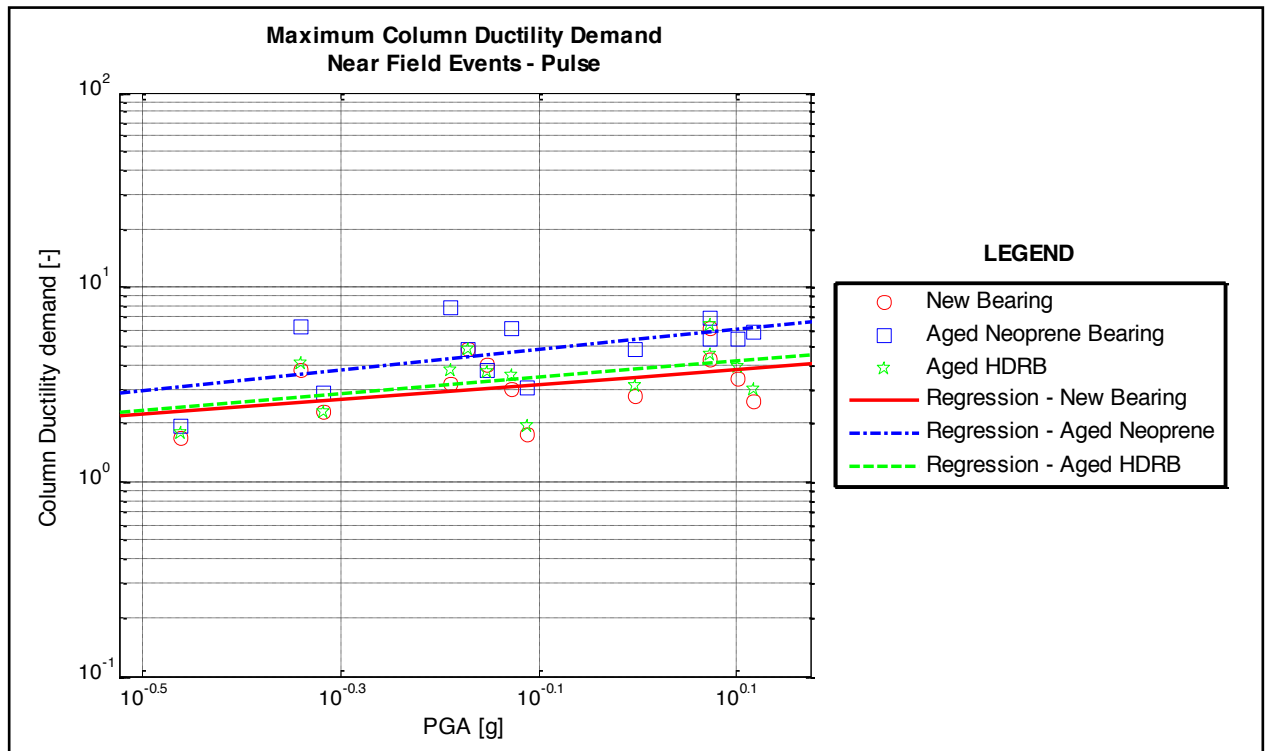


Figure 45. Peak Column Ductility Demand vs. PGA (NF-pulse record set)

---

## V. CONCLUSIONS

The aims of this research included (i) examining the effects of aging on the axial and shear response of FRBs, and (ii) verifying the effects of aging in rubber-based devices on the seismic response a typical base isolated bridge in California. To determine the effects of aging on the response of FRBs under a variety of loading conditions, thermal oxidation tests were performed and results of the tests were compared to those available in literature for conventional steel reinforced devices. From the results of the tests, we can conclude the following:

1. FRBs can be produced to exhibit limited run-in effects when loaded in compression;
2. FRBs tested to low levels of lateral deformation (i.e., 50% shear strain) have a negligible degradation of the force displacement response. For larger levels of deformation (i.e., shear strains larger than 75%), the measured hysteresis response shows degradation and a softening of the devices after a few cycles of imposed displacements. This softening response is associated with damage of the tested samples at the interfaces between the layers of elastomer and layers of fiber.
3. For the tested bearings, at 50% shear strain, an equivalent viscous damping between 12% to 16% of critical was measured. This result is in line with the findings of Kelly.<sup>11</sup> An increase in EDC was measured with aging.
4. A variation of oven aging time in the range of 0–6 weeks causes a variation of horizontal stiffness (i.e., effective shear modulus) of 41% at 50% shear strain.
5. Under each level of imposed lateral deformations, the larger load-resisting capacity and damping were observed during the first cycles of deformation. For the following cycles of hysteresis at 50% shear strain, the bearings exhibited a stable hysteretic response.
6. Results of the tests performed on FRBs were compared to those obtained for steel reinforced elastomeric devices described in Report 449.<sup>25</sup> The tests show that after 6 weeks of curing, the variation of lateral stiffness of FRBs is larger than that of steel reinforced devices.

It is clear that the tests reported in this study are not sufficient for a full comparison of the response of FRBs against conventional elastomeric bearings. The high degradation of FRBs measured from the tests could be due to the manufacturing of the samples or to the type of elastomer or fibers in use. For a full understanding of any significant difference between the aging of conventional devices and fiber reinforced devices, it is necessary to test bearings produced by the same manufacturer (*i.e.*, same quality and production process). The influence of different types of reinforcements on the aging response of FRBs should additionally be assessed. In the second part of this research work, the aged response of elastomeric bearings has been included in a full model of a bridge representative of a typical overpass structure in California. A comparison of the performance of the fixed base model versus the response of the base isolated model is not disused in this work. If the readers are interested in such a comparison, they can find a detailed analysis in Aviram.

This study has examined the force and deformation demands on key components of the bridge when new and aged responses of elastomeric devices are considered. Results of NRHAs performed in SAP 2000 were plotted against period independent intensity measures (IMs), and data was fitted using a power trendline. Because of the many outliers, these regression lines do not fit the data well. For this reason, the results of the analyses only provide a general information on the tendency of the response of the bridge. These lines are not exact relations between the IMs and the EDPs. From the results of the numerical analyses, the following conclusions can be drawn:

1. The deformation demand on the bearings reduces significantly due to devices aging. This effect is more pronounced for neoprene bearings than for HDNRBs.
2. As aged bearings are stiffer than new isolators, the efficiency of base isolation reduces with time. The increase in force demand on the column of the bridge is more pronounced for neoprene devices than for HDNRBs.
3. The aging of the isolators has a negligible effect on the vertical acceleration of the deck. This is true for all the intensity levels and for NF-pulse motions as well.
4. The aging of the elastomeric devices seems to have a negligible effect on the axial load on passive devices.
5. The column ductility demand and the top column rotation increases with aging of the bearings. This effect is more pronounced under near field events than under far field ones.

It should be noted that aging effects were included in this model as modification factors for the lateral response of the bearings. Additional analyses are required to assess the effects of aging on the vertical response of the devices and on EDPs descriptive of the response of components of the bridge under multidirectional excitations.

---

## ABBREVIATIONS AND ACRONYMS

---

AASHTO	American Association of State Highway and Transportation Officials
EDC	Energy Dissipated per Cycle
EDP	Engineering Demand Parameter
FRB	Fiber Reinforced Bearing
HDRB	High Damping Rubber Bearing
IM	Intensity Measure
LRB	Laminated Rubber Bearing
MTI	Mineta Transportation Institute
NE	Neoprene Rubber
NR	Natural Rubber
NRHA	Nonlinear Response History Analysis
PGA	Peak Ground Acceleration
PGD	Peak Ground Displacement
PGV	Peak Ground Velocity

---

---

## ENDNOTES

1. H. Nakauchi, "Characterization of a 100-years-old Rubber Bearing by Microanalytical Methods." *Journal of Applied Polymer Science, Applied Polymer Symposium* 50 (1992): 369–375.
2. Wise, J., K. T. Gillen, and R. L. Clough. "An ultrasensitive technique for testing the Arrhenius extrapolation assumption for thermally aged elastomers." *Polymer Degradation and Stability* 49, no. 3 (1995): 403–418.
3. Watanabe, Y., A. Kato, G. Yoneda, and T. Hirotsu. "Aging effects of forty years old laminated rubber bearings." In *Proc. 1st Aseismic and Resist Colloquium, JSCE*, pp. 439–446. 1996.
4. Celina, M., J. Wise, D. K. Ottesen, K. T. Gillen, and R. L. Clough. "Correlation of chemical and mechanical property changes during oxidative degradation of neoprene." *Polymer degradation and Stability* 68, no. 2 (2000): 171–184.
5. Itoh, Yoshito, Haosheng Gu, Kazuya SATOH, and Yukihiro KUTSUNA. "Experimental investigation on ageing behaviors of rubbers used for bridge bearings." *Doboku Gakkai Ronbunshuu A* 62, no. 1 (2006): 176–190.
6. Itoh, Yoshito, Haosheng Gu, Kazuya Satoh, and Yoshihisa Yamamoto. "Long-term deterioration of high damping rubber bridge bearing." *Doboku Gakkai Ronbunshuu A* 62, no. 3 (2006): 595–607.
7. Hamaguchi, Hiroki, Satoru Aizawa, Yusuke Samejima, Takashi Kikuchi, Shigenobu Suzuki, and Toshikazu Yoshizawa. "A study of aging effect on a rubber bearing after about twenty years in use." *AIJ Journal of Technology and Design* 15, no. 30 (2009): 393–398.
8. Choun, Young-Sun, Junhee Park, and In-Kil Choi. "Effects of mechanical property variability in lead rubber bearings on the Response of seismic isolation system for different ground motions." *Nuclear Engineering and Technology* 46, no. 5 (2014): 605–618.
9. Kelly, James M. "Analysis of fiber-reinforced elastomeric isolators." *Journal of Seismology and Earthquake Engineering* 2, no. 1 (1999): 19–34.
10. Moon, Byung-Young, Gyung-Ju Kang, Beom-Soo Kang, and James M. Kelly. "Design and manufacturing of fiber reinforced elastomeric isolator for seismic isolation." *Journal of Materials Processing Technology* 130 (2002): 145–150.
11. Al-Anany, Yasser M., and Michael J. Tait. "Fiber reinforced elastomeric isolators for the seismic isolation of bridges." *Composite Structures* 160 (2017): 300–311.
12. Kelly, James M., and Andrea Calabrese. *Mechanics of fiber reinforced bearings*. Berkeley, CA: Pacific Earthquake Engineering Research Center, 2012.

13. Spizzuoco, Mariacristina, Andrea Calabrese, and Giorgio Serino. “Innovative low-cost recycled rubber–fiber reinforced isolator: experimental tests and finite element analyses.” *Engineering Structures* 76 (2014): 99–111.
14. Al-Anany, Yasser M., and Michael J. Tait. “Experimental assessment of utilizing fiber reinforced elastomeric isolators as bearings for bridge applications.” *Composites Part B: Engineering* 114 (2017): 373–385.
15. Calabrese, Andrea, Mariacristina Spizzuoco, Giorgio Serino, Gaetano Della Corte, and Giuseppe Maddaloni. “Shaking table investigation of a novel, low-cost, base isolation technology using recycled rubber.” *Structural Control and Health Monitoring* 22, no. 1 (2015): 107–122.
16. Dezfuli, F. Hedayati, and M. Shahria Alam. “Multi-criteria optimization and seismic performance assessment of carbon FRP-based elastomeric isolator.” *Engineering Structures* 49 (2013): 525–540.
17. Russo, Gaetano, Margherita Pauletta, and Andrea Cortesia. “A study on experimental shear behavior of fiber-reinforced elastomeric isolators with various fiber layouts, elastomers and aging conditions.” *Engineering Structures* 52 (2013): 422–433.
18. Russo, G., Pauletta, M. and Cortesia, A., 2013. A study on experimental shear behavior of fiber-reinforced elastomeric isolators with various fiber layouts, elastomers and aging conditions. *Engineering Structures*, 52, pp. 422–433.
19. Buckle, Ian G., Michael C. Constantinou, Mirat Diceli, and Hamid Ghasemi. *Seismic isolation of highway bridges*. No. MCEER-06-SP07. 2006.
20. Micelli, F., and A. Nanni. “Tensile characterization of FRP rods for reinforced concrete structures.” *Mechanics of composite materials* 39, no. 4 (2003): 293–304.
21. Itoh, Y., and H. S. Gu. “Prediction of aging characteristics in natural rubber bearings used in bridges.” *Journal of Bridge Engineering* 14, no. 2 (2009): 122–128.
22. AASHTO M251-06, *Standard Specification for Plain and Laminated Elastomeric Bridge Bearings*, American Association of State and Highway Transportation Officials, 2016.
23. ASTM D 573-04, *Test Method for Rubber-Deterioration in an Air Oven*, American Society for Testing and Materials, 2004.
24. Yura, J., Kumar, A., Yakut, A., Topkaya, C., Becker, E. and Collingwood, J., 2001. *Elastomeric bridge bearings: Recommended test methods* (No. Project D10-51 FY’97).
25. ISO 4587:2003, *Adhesives—Determination of tensile lap-shear strength of rigid-to-rigid bonded assemblies*, 2003

26. Gent, A. N. "Compression of rubber blocks." *Rubber chemistry and technology* 67, no. 3 (1994): 549–558.
27. Kelly, James. "Analysis of the run-in effect in fiber-reinforced isolators under vertical load." *Journal of Mechanics of Materials and Structures* 3, no. 7 (2008): 1383–1401.
28. Grant, Damian N., Gregory L. Fenves, and Ferdinando Auricchio. "Bridge isolation with high-damping rubber bearings—analytical modelling and system response." In *13th World Conference on Earthquake Engineering Vancouver, BC*. 2004.
29. Gent, Alan N. *Engineering with rubber: how to design rubber components*. Carl Hanser Verlag GmbH Co KG, 2012.
30. Thompson, Andrew CT, Andrew S. Whittaker, Gregory L. Fenves, and Stephen A. Mahin. "Property modification factors for elastomeric seismic isolation bearings." In *Proceedings of the 12th World Conference on Earthquake Engineering*. Upper Hutt, NZ: New Zealand Society for Earthquake Engineering, 2000.
31. Aviram, A., A. Schellenberg, and Božidar Stojadinovic. "Seismic Design and performance of two isolation systems used for reinforced concrete bridge construction." In *Proceedings of the 15th World Conference on Earthquake Engineering*. 2012.
32. Ketchum, Mark, Vivian Chang, James Scheld, Kwong Cheng, Francis Drouillard, Thomas Shantz, and Fadel Alemmedine. "Influence of design ground motion level on highway bridge costs." Report No. Lifelines 6D01 (2004).
33. Aviram Traubita, Ady. "Structural Response and Cost Characterization of Bridge Construction using Seismic Performance Enhancement Strategies." PhD diss., UC Berkeley, 2009.
34. AASHTO 1996, *Standard Specifications for Highway Bridges*, American Association of State and Highway Transportation Officials, 1996.
35. CALTRANS, *Seismic Design Criteria Seismic Design Criteria, VERSION 1.3*, 2004.
36. Aviram, Ady, Kevin Rory Mackie, and Božidar Stojadinović. *Guidelines for nonlinear analysis of bridge structures in California*. Pacific Earthquake Engineering Research Center, 2008.
37. AASHTO 1999, *Guide Specifications for Seismic Isolation Design*, American Association of State and Highway Transportation Officials, 1999.
38. Yang, T. Y., Dimitrios Konstantinidis, and James M. Kelly. "The influence of isolator hysteresis on equipment performance in seismic isolated buildings." *Earthquake Spectra* 26, no. 1 (2010): 275–293.
39. Kelly, James M., and Dimitrios Konstantinidis. *Mechanics of rubber bearings for seismic and vibration isolation*. John Wiley & Sons, 2011.

- 
40. Constantinou, Michalakis C., Panos Tsopelas, Amarnath Kasalanati, and Eric D. Wolff. "Property modification factors for seismic isolation bearings." (1999).
  41. Thompson, Andrew CT, Andrew S. Whittaker, Gregory L. Fenves, and Stephen A. Mahin. "Property modification factors for elastomeric seismic isolation bearings." In Proceedings of the 12th World Conference on Earthquake Engineering. Upper Hutt, NZ: New Zealand Society for Earthquake Engineering, 2000.
  42. AASHTO 2014, Guide Specifications for LRFD Seismic Bridge Design, American Association of State and Highway Transportation Officials, 2014.
  43. Applied Technology Council. Quantification of building seismic performance factors. US Department of Homeland Security, FEMA, 2009.
  44. Glantz, Stanton A., Bryan K. Slinker, and Torsten B. Neilands. Primer of applied regression and analysis of variance. Vol. 309. New York: McGraw-Hill, 1990.

---

## BIBLIOGRAPHY

- AASHTO 1999, Guide Specifications for Seismic Isolation Design. American Association of State and Highway Transportation Officials, 1999.
- AASHTO 20014, Guide Specifications for LRFD Seismic Bridge Design American Association of State and Highway Transportation Officials, 2014.
- AASHTO 1996, Standard Specifications for Highway Bridges, American Association of State and Highway Transportation Officials, 1996.
- AASHTO M251-06, Standard Specification for Plain and Laminated Elastomeric Bridge Bearings. American Association of State and Highway Transportation Officials, 2016.
- Al-Anany, Yasser M., and Michael J. Tait. "Experimental assessment of utilizing fiber reinforced elastomeric isolators as bearings for bridge applications." *Journal of Composites Part B: Engineering* 114 (2017): 373–385.
- Al-Anany, Yasser M., and Michael J. Tait. "Fiber reinforced elastomeric isolators for the seismic isolation of bridges." *Journal of Composite Structures* 160 (2017): 300–311.
- Applied Technology Council. Quantification of building seismic performance factors. US Department of Homeland Security, FEMA, 2009.
- Aviram Traubita, Ady, Andreas Schellenberg, and Bozidar Stojadinovic. "Seismic Design and performance of two isolation systems used for reinforced concrete bridge construction." Paper presented at the 15th World Conference on Earthquake Engineering, 2012.
- Aviram Traubita, Ady, Kevin Rory Mackie, and Božidar Stojadinović. *Guidelines for Nonlinear Analysis of Bridge Structures in California*. Berkeley, CA: Pacific Earthquake Engineering Research Center, 2008.
- Aviram Traubita, Ady. *Structural Response and Cost Characterization of Bridge Construction using Seismic Performance Enhancement Strategies*. Berkeley, CA: University of Berkeley, 2009.
- ASTM D 573-04(2015). *Standard Test Method for Rubber—Deterioration in an Air Oven*. West Conshohocken, PA: American Society of Testing and Materials, 2004.
- Buckle, Ian G., Michael C. Constantinou, Mirat Diceli, and Hamid Ghasemi. *Seismic Isolation of Highway Bridges*. No. MCEER-06-SP07. 2006.

- Calabrese, Andrea, Mariacristina Spizzuoco, Giorgio Serino, Gaetano Della Corte, and Giuseppe Maddaloni. "Shaking table investigation of a novel, low-cost, base isolation technology using recycled rubber." *Journal of Structural Control and Health Monitoring* 22, no. 1 (2015): 107–122.
- CALTRANS, *Seismic Design Criteria*. Version 1.3, 2004.
- Celina, Mathias C., Jonathan L. Wise, David K. Ottesen, Kenneth T. Gillen, and Roger L. Clough. "Correlation of chemical and mechanical property changes during oxidative degradation of neoprene." *Journal of Polymer degradation and Stability* 68, no. 2 (2000): 171–184.
- Choun, Young-Sun, Junhee Park, and In-Kil Choi. "Effects of mechanical property variability in lead rubber bearings on the Response of seismic isolation system for different ground motions." *Journal of Nuclear Engineering and Technology* 46, no. 5 (2014): 605–618.
- Constantinou, Michalakis C., Panos Tsopelas, Amarnath Kasalanati, and Eric D. Wolff. *Property Modification Factors for Seismic Isolation Bearings*. Technical Report MCEER-99-0012, 1999.
- Dezfuli, Farshad Hedayati, and M. Shahria Alam. "Multi-criteria Optimization and Seismic Performance Assessment of Carbon FRP-based Elastomeric Isolator." *Journal of Engineering Structures* 49 (2013): 525–540.
- Gent, Alan N. "Compression of rubber blocks." *Journal of Rubber chemistry and technology* 67, no. 3 (1994): 549–558.
- Gent, Alan N. *Engineering with Rubber: How to Design Rubber Components*. Munich, Germany: Carl Hanser Verlag GmbH & Co. KG, 2012.
- Glantz, Stanton A., Bryan K. Slinker, and Torsten B. Neilands. *Primer of applied regression and analysis of variance*. Vol. 309. New York: McGraw-Hill, 1990.
- Grant, Damian N., Gregory L. Fenves, and Ferdinando Auricchio. "Bridge isolation with high-damping rubber bearings—analytical modelling and system response." Paper presented at The 13th World Conference on Earthquake Engineering, Vancouver, Canada, August 1-6, 2004.
- Hamaguchi, Hiroki, Satoru Aizawa, Yusuke Samejima, Takashi Kikuchi, Shigenobu Suzuki, and Toshikazu Yoshizawa. "A study of aging effect on a rubber bearing after about twenty years in use." *AIJ Journal of Technology and Design* 15, no. 30 (2009): 393–398.
- Itoh, Yoshito, Haosheng Gu, Kazuya Satoh, and Yukihiro Kutsuna. "Experimental investigation on ageing behaviors of rubbers used for bridge bearings." *Doboku Gakkai Ronbunshuu A* 62, no. 1 (2006): 176–190.

- Itoh, Yoshito, Haosheng Gu, Kazuya Satoh, and Yoshihisa Yamamoto. "Long-term deterioration of high damping rubber bridge bearing." *Doboku Gakkai Ronbunshuu A* 62, no. 3 (2006): 595–607.
- Itoh, Yoshito, and Haosheng Gu. "Prediction of aging characteristics in natural rubber bearings used in bridges." *Journal of Bridge Engineering* 14, no. 2 (2009): 122–128.
- ISO 4587:2003, *Adhesives – Determination of Tensile Lap-Shear Strength of Rigid-to-Rigid Bonded Assemblies*. International Organization for Standardization, 2003.
- Kelly, James M. "Analysis of fiber-reinforced elastomeric isolators." *Journal of Seismology and Earthquake Engineering* 2, no. 1 (1999): 19–34.
- Kelly, James M. "Analysis of the run-in effect in fiber-reinforced isolators under vertical load." *Journal of Mechanics of Materials and Structures* 3, no. 7 (2008): 1383–1401.
- Kelly, James M., and Andrea Calabrese. *Mechanics of fiber reinforced bearings*. Berkeley, CA: Pacific Earthquake Engineering Research Center, 2012.
- Kelly, James M., and Dimitrios Konstantinidis. *Mechanics of rubber bearings for seismic and vibration isolation*. John Wiley & Sons, 2011.
- Ketchum, Mark, Vivian Chang, James Scheld, Kwong Cheng, Francis Drouillard, Thomas Shantz, and Fadel Aledmeddine. *Influence of Design Ground Motion Level on Highway Bridge Costs*. Berkeley, CA: Pacific Earthquake Engineering Research Center, 2004.
- Micelli, Francesco, and Antonio Nanni. "Tensile characterization of FRP rods for reinforced concrete structures." *Journal of Mechanics of composite materials* 39, no. 4 (2003): 293–304.
- Moon, Byung-Young, Gyung-Ju Kang, Beom-Soo Kang, and James M. Kelly. "Design and manufacturing of fiber reinforced elastomeric isolator for seismic isolation." *Journal of Materials Processing Technology* 130 (2002): 145–150.
- Nakauchi, H. "Characterization of a 100-years-old Rubber Bearing by Microanalytical Methods." *Journal of Applied Polymer Science, Applied Polymer Symposium* 50 (1992): 369–375.
- Russo, Gaetano, Margherita Pauletta, and Andrea Cortesia. "A study on experimental shear behavior of fiber-reinforced elastomeric isolators with various fiber layouts, elastomers and aging conditions." *Engineering Structures* 52, pp.422–433.
- Spizzuoco, Mariacristina, Andrea Calabrese, and Giorgio Serino. "Innovative low-cost recycled rubber–fiber reinforced isolator: experimental tests and finite element analyses." *Engineering Structures* 76 (2014): 99–111.

- 
- Thompson, Andrew CT, Andrew S. Whittaker, Gregory L. Fenves, and Stephen A. Mahin. "Property modification factors for elastomeric seismic isolation bearings." Paper presented at The 12th World Conference on Earthquake Engineering, Auckland, New Zealand, January 30-February 4, 2000.
- Watanabe, Y., A. Kato, Karl G. Yoneda, and T. Hirotsu. "Aging effects of forty years old laminated rubber bearings." In *Proc. 1st Aseismic and Resist Colloquium*, pp. 439–446. Japan Society of Civil Engineers, 1996.
- Wise, Jonathan L., Kenneth T. Gillen, and Roger L. Clough. "An ultrasensitive technique for testing the Arrhenius extrapolation assumption for thermally aged elastomers." *Journal of Polymer Degradation and Stability* 49, no. 3 (1995): 403–418.
- Yang, Tony, Dimitrios Konstantinidis, and James M. Kelly. "The influence of isolator hysteresis on equipment performance in seismic isolated buildings." *Journal of Earthquake Spectra* 26, no. 1 (2010): 275–293.
- Yura, Joseph A., Alok Kumar, Ahmet Yakut, Cem Topkaya, Eric Becker, and Jerry P. Collingwood. *Elastomeric bridge bearings: Recommended test methods*. National Cooperative Highway Research Program Report 449, 2001.

## ABOUT THE AUTHORS

### **ANDREA CALABRESE, PHD, ING, CENG, MICE**

Dr. Calabrese joined the CSULB CECEM Department as an Assistant Professor in Fall 2017. He gained a Ph.D. in Construction Engineering with an emphasis in Structural Engineering in 2013. He was a visiting research fellow at the Pacific Earthquake Engineering Research Center (PEER) from 2010–2012 along with having been a postdoctoral researcher of the ReLUIS Consortium at the Italian Network of University Laboratories in Earthquake Engineering, from 2013–2014. Dr. Calabrese has worked as a Structural Engineer at Foster & Partners, London and Italy for seven years. He has been a registered engineer in Italy since 2009 and a Chartered Engineer (CEng) and Full Member of the Institution of Civil Engineers (MICE) in the UK since 2017. Dr. Calabrese's current research interests are in the fields of experimental testing, structural dynamics, base isolation, vibration engineering, and in the development of novel low-cost devices for the seismic protection of buildings. He has carried out numerous large-scale experimental studies of base isolation systems and energy-absorbing devices on the shaking table at the Department of Structural Engineering at the University of Naples in Italy. This work has been instrumental in developing low-cost seismic isolation systems using recycled rubber and flexible reinforcements for the seismic protection of buildings in developing regions.

### **ARMAN BARJANI**

Arman Barjani is a graduate student at the CSULB CECEM Department. His responsibilities have included running the Nonlinear Response History Analyses described in this study.

### **NGHIEM TRAN**

Nghiem Tran is an undergraduate student at the CSULB CECEM Department. His responsibilities have included performing this study's experimental tests.

## **PEER REVIEW**

San José State University, of the California State University system, and the MTI Board of Trustees have agreed upon a peer review process required for all research published by MTI. The purpose of the review process is to ensure that the results presented are based upon a professionally acceptable research protocol.

## MTI BOARD OF TRUSTEES

**Founder, Honorable Norman Mineta (Ex-Officio)**  
Secretary (ret.),  
US Department of Transportation

**Chair, Grace Crunican (TE 2019)**  
General Manager  
Bay Area Rapid Transit District (BART)

**Vice Chair, Abbas Mohaddes (TE 2021)**  
President & COO  
Econolite Group Inc.

**Executive Director, Karen Philbrick, Ph.D. (Ex-Officio)**  
Mineta Transportation Institute  
San José State University

**Richard Anderson (Ex-Officio)**  
President & CEO  
Amtrak

**Laurie Berman (Ex-Officio)**  
Director  
California Department of Transportation (Caltrans)

**David Castagnetti (TE 2021)**  
Co-Founder  
Mehlman Castagnetti  
Rosen & Thomas

**Maria Cino (TE 2021)**  
Vice President  
America & U.S. Government  
Relations Hewlett-Packard Enterprise

**Donna DeMartino (TE 2021)**  
General Manager & CEO  
San Joaquin Regional Transit District

**Nuria Fernandez\* (TE 2020)**  
General Manager & CEO  
Santa Clara Valley  
Transportation Authority (VTA)

**John Flaherty (TE 2020)**  
Senior Fellow  
Silicon Valley American  
Leadership Form

**Rose Guilbault (TE 2020)**  
Board Member  
Peninsula Corridor  
Joint Powers Board

**Ian Jefferies (Ex-Officio)**  
President & CEO  
Association of American Railroads

**Diane Woodend Jones (TE 2019)**  
Principal & Chair of Board  
Lea + Elliott, Inc.

**Will Kempton (TE 2019)**  
Retired

**Jean-Pierre Loubinoux (Ex-Officio)**  
Director General  
International Union of Railways (UIC)

**Bradley Mims (TE 2020)**  
President & CEO  
Conference of Minority  
Transportation Officials (COMTO)

**Jeff Morales (TE 2019)**  
Managing Principal  
InfraStrategies, LLC

**Dan Moshavi, Ph.D. (Ex-Officio)**  
Dean, Lucas College and  
Graduate School of Business  
San José State University

**Takayoshi Oshima (TE 2021)**  
Chairman & CEO  
Allied Telesis, Inc.

**Paul Skoutelas (Ex-Officio)**  
President & CEO  
American Public Transportation  
Association (APTA)

**Dan Smith (TE 2020)**  
President  
Capstone Financial Group, Inc.

**Beverly Swaim-Staley (TE 2019)**  
President  
Union Station Redevelopment  
Corporation

**Larry Willis (Ex-Officio)**  
President  
Transportation Trades  
Dept., AFL-CIO

**Jim Thymon (Ex-Officio)**  
Executive Director  
American Association of  
State Highway and Transportation  
Officials (AASHTO)  
[Retiring 12/31/2018]

(TE) = Term Expiration  
\* = Past Chair, Board of Trustees

## Directors

**Karen Philbrick, Ph.D.**  
Executive Director

**Hilary Nixon, Ph.D.**  
Deputy Executive Director

**Asha Weinstein Agrawal, Ph.D.**  
Education Director  
National Transportation Finance  
Center Director

**Brian Michael Jenkins**  
National Transportation Security  
Center Director

## Research Associates Policy Oversight Committee

**Jan Botha, Ph.D.**  
Civil & Environmental Engineering  
San José State University

**Katherine Kao Cushing, Ph.D.**  
Environmental Science  
San José State University

**Dave Czerwinski, Ph.D.**  
Marketing and Decision Science  
San José State University

**Frances Edwards, Ph.D.**  
Political Science  
San José State University

**Taeho Park, Ph.D.**  
Organization and Management  
San José State University

**Christa Bailey**  
Martin Luther King, Jr. Library  
San José State University